Therapeutics

FORUM REVIEW ARTICLE

Exploiting Oxidative Microenvironments in the Body as Triggers for Drug Delivery Systems

Shivanjali Joshi-Barr,[1] Caroline de Gracia Lux,[1] Enas Mahmoud,[1,*] and Adah Almutairi[1,2]

Abstract

Significance: Reactive oxygen species and reactive nitrogen species (ROS/RNS) play an important role in cell signaling pathways. However, the increased production of these species may disrupt cellular homeostasis, giving rise to pathological conditions. Biomaterials that are responsive to ROS/RNS can be strategically used to specifically release therapeutics and diagnostic agents to regions undergoing oxidative stress. *Recent Advances:* Many nanocarriers intended to exploit redox micro-environments as triggers for drug release, summarized and compared in this review, have recently been developed. We describe these carriers' chemical structures, strategies for payload protection and oxidation-selective release, and ROS/RNS sensitivity as tested in initial studies. *Critical Issues:* ROS/RNS are unstable, so reliable measures of their concentrations in various conditions are scarce. Combined with the dearth of materials shown to respond to physiologically relevant levels of ROS/RNS, evaluations of their true sensitivity are difficult. *Future Directions:* Oxidation-responsive nanocarriers developed thus far show tremendous potential for applicability *in vivo*; however, the sensitivity of these chemistries needs to be fine tuned to enable responses to physiological levels of ROS and RNS. *Antioxid. Redox Signal.* 21, 730–754.

Introduction

REACTIVE OXYGEN SPECIES (ROS) and reactive nitrogen species (RNS) found in living organisms are produced as by-products of biochemical reactions occurring within the cell. Some of the most common ROS and RNS include H_2O_2 (hydrogen peroxide), $O_2^{\bullet-}$ (superoxide), $^{\bullet}OH$ (hydroxyl radical), OCl^- (hypochlorite ion), NO (nitric oxide), and $ONOO^-$ (peroxynitrite). Due to their inherently reactive nature, ROS and RNS degrade rapidly by interacting with surrounding molecules, covalently modifying them. Antioxidants such as glutathione (GSH), citrulline, vitamin E, and polyphenols, along with enzymes such as superoxide dismutase (SOD), catalase, and GSH peroxidase (GPX), scavenge and quench ROS (158). At low physiological levels of ROS and RNS, chemically modified biomolecules (proteins and lipids) serve as key modulators of intra- and extracellular signaling pathways [extensively reviewed in (42, 57, 180, 182)]. At higher levels, ROS and RNS give rise to oxidative stress, a condition in which ROS/RNS concentrations exceed cells' antioxidant capacity. While oxidative stress is beneficial in processes such as inflammation (*e.g.*, immune cell-mediated destruction of microbial agents), it can also be detrimental to cells, as it induces irreversible changes to biomolecules. These changes, such as carbonylation, glycation, S-glutathiolation, and S-nitrosylation of proteins, have been implicated in the pathogenesis of diseases, including Alzheimer's and diabetic complications (24, 128, 151). Altered ROS regulation as a result of aging (108) may contribute to increased risk for oxidative stress-associated disorders. Lipids of cellular membranes are also damaged by oxidative conditions, giving rise to unstable lipid hydroperoxides (9). Chronic oxidative stress promotes breaks in double-stranded DNA [especially mitochondrial DNA (mtDNA)], leading to mutations linked with mitochondrial disorders (97). Chronic oxidative stress is, thus, considered an important contributing factor to the etiology of diseases such as cancer, neurodegeneration, and cardiovascular dysfunction.

[1]Skaggs School of Pharmacy and Pharmaceutical Sciences, Laboratory of Bioresponsive Materials, University of California, San Diego, San Diego, California.
[2]KACST-UCSD Center for Excellence in Nanomedicine and Engineering (Institute of Engineering in Medicine), Laboratory of Bioresponsive Materials, University of California, San Diego, San Diego, California.
*Current affiliation: Department of Pharmaceutics, Faculty of Pharmacy, Cairo University, Cairo, Egypt.

The unique redox microenvironment of cells and tissues experiencing oxidative stress can be exploited for the delivery of therapeutics and diagnostics agents *via* nanoscale carriers that are tailored to release their contents in conditions of oxidative stress. Current chemical mechanisms involved in biomaterials with potential of ROS-induced degradation or release have been reviewed in detail in a recent review (112). Drug delivery *via* nanoparticles promises to revolutionize human health by broadening the range of usable drugs and, with disease-specific engineering, reducing dosages and limiting side effects. Nanoparticles with hydrophobic cores enable the delivery of drugs that are poorly water soluble, which are otherwise difficult to administer intravenously at effective concentrations; other nanoscale formulations enable the delivery of proteins or peptides that are sensitive to proteolytic degradation, if left unprotected. The second advantage lies in the large surface area of nanoparticles, which enables the attachment of many antibodies, aptamers, or peptides that promote uptake by tissues or tumors that overexpress their cognate receptors, concentrating imaging signals or minimizing drug side effects. Using a slightly different approach, ''bioresponsive'' nanovehicles can be customized to respond to a stimulus (either characteristic of disease, for example, acidic pH, or user controlled, for example, near infrared light) by releasing cargo. Oxidation-sensitive nanovehicles, therefore, represent such a class of ''smart'' drug carriers that should target the delivery of therapeutics and diagnostic agents to regions experiencing high oxidative stress. To achieve this goal, potential ROS-responsive carriers may incorporate one of several strategies to translate a reaction with ROS to macroscopic physical changes in the nanocarrier that enable the release of contents. Such strategies include degradation, leading to swelling and dissolution of the carrier or a switch from hydrophobic to hydrophilic character of the nanocarrier material, causing complex disassociation.

In this review, we first briefly describe cellular sources of ROS/RNS and pathological conditions arising from oxidative stress. In order to explain the challenges inherent in assessing the sensitivity of ROS-responsive nanocarriers, we then discuss strategies for measuring ROS/RNS. Finally, we present a summary of the various chemical systems (micelles, polymeric nano/microparticles, and supramolecular hydrogels) developed to date that can respond to altered oxidative microenvironments.

Cellular Sources of ROS/RNS

Diseases involving oxidative stress result from alterations in cellular mechanisms regulating redox homeostasis. In order to design strategies to combat oxidative stress or to harness the unique redox microenvironments for the purpose of drug delivery, it is important to understand the cellular sources of ROS/RNS in order to ensure that they reach the appropriate subcellular location. Some of the main organelles involved in ROS/RNS production are described next, along with the enzymes involved in ROS/RNS production and scavenging (Table 1).

Mitochondria

Mitochondria are the primary sites for oxygen metabolism and account for the consumption of 85%–90% of cellular oxygen (161). Mitochondrial respiration produces primarily superoxide and hydrogen peroxide. Superoxide radicals are produced by Complex I and III of the electron transport chain (ETC) in the intermembrane space (15, 181) and ETC flavoproteins in the matrix (168). Superoxide is scavenged by the manganese SOD2 in the mitochondrial matrix to produce H_2O_2, which can freely diffuse across membrane bilayers (193). Another source of cytosolic H_2O_2 is monoamine oxidase, a non-ETC enzyme that metabolizes neurotransmitters and dietary monoamines, which are present in the mitochondrial outer membrane (163). This H_2O_2 is consumed in the cytosol by catalase (67) and in the mitochondria, by GPX and thioredoxin peroxidase (27, 56). Alternatively, H_2O_2 can react with iron clusters that are abundant in the mitochondria *via* Fenton chemistry to form hydroxyl radicals (71).

Mitochondria also contribute to the production of RNS, also potent oxidizers, by the action of mitochondrial nitric oxide synthase (mtNOS), which produces nitric oxide (NO) (59). Nitric oxide can react with mitochondrial superoxide and produce peroxynitritite ($ONOO^-$) (59). Peroxynitrite can oxidize proteins, especially mitochondrial enzymes such as the components of the ETC and SOD2, or cause calcium release, changing mitochondrial permeability (59).

Oxidative stress from mitochondrial dysfunction has been linked to several neurological disorders such as Alzheimer's and Parkinson's (see next section for their pathophysiology). Some of these disorders result from dysfunction of non-mitochondrial proteins; for example, in Friedreich's ataxia, mutations in an iron-binding protein cause mitochondrial iron overload, which damages mitochondrial proteins that usually reduce ROS (197). Other rare diseases result from mutations in the mitochondrial DNA (mtDNA) that affect the function of ETC, which cause respiratory defects and enhanced ROS production (174).

Peroxisomes

Peroxisomes are specialized organelles that function primarily in the catabolism of long-chained and branched-chain fatty acids by β-oxidation. Peroxisomal enzymes also detoxify and metabolize compounds that are poorly soluble in water and lipids (5). The primary ROS byproduct of peroxisomal enzymes (*e.g.*, acyl CoA oxidase, urate oxidase, and amino acid oxidase) is H_2O_2; however, superoxide and nitric oxide are also produced by xanthine oxidase and NO synthase, respectively (5). To protect against oxidants, peroxisomes also contain enzymes that scavenge ROS. These include catalase, SOD, peroxiredoxin, epoxide hydrolase, GSH S-transferase, and several peroxisome-specific integral membrane proteins (peroxisomal membrane protein 2, Mpv-17, and Mpv-like protein) (5). If peroxisome proliferation is stimulated (*e.g.*, by pharmacological agents) or peroxisomal ROS-scavenging enzymes are mutated, this results in excessive ROS production and oxidative stress, which may lead to disease. Imbalances in the homeostasis of ROS in peroxisomes have been linked to diseases such as cancer, neurodegeneration, and type 2 diabetes (61).

Plasma membrane/extracellular space and phagosome

ROS are also produced to combat infectious disease: Phagocytes, especially neutrophils and monocytes, rapidly

TABLE 1. ENZYMES INVOLVED IN THE PRODUCTION OR CONSUMPTION OF REACTIVE
OXYGEN SPECIES AND REACTIVE NITROGEN SPECIES

Enzyme	Reaction	Localization and tissue abundance	Ref.
Copper-zinc superoxide dismutase (Cu/ZnSOD or SOD1)	$2O_2^{\bullet-} + 2H^+ \rightarrow O_2 + H_2O_2$	Cytoplasm, nucleus, lysosomes, and mitochondria	(31, 63, 129, 147)
Manganese SOD (MnSOD or SOD2)		Mostly mitochondria	(92, 164, 193)
Extracellular SOD (ECSOD or SOD3)		Extracellular space; 10 times higher activity in vascular walls	(65, 170)
Catalase	$2H_2O_2 \rightarrow 2H_2O + O_2$	Peroxisomes; mostly in liver parenchyma and renal proximal tubule	(29, 30, 86)
Myeloperoxidase (MPO)	$H_2O_2 + Cl^- \rightarrow HOCl + OH^-$	Lysosomes of polymorphonuclear neutrophils	(96, 99)
Glutathione peroxidase	$2GSH + H_2O_2 \rightarrow GS\text{-}SG + 2H_2O$	GPX1, cytoplasm of most tissues; GPX3, plasma	(7, 35, 36, 133, 173)
Xanthine oxidase	$Xanthine + H_2O + O_2 \rightarrow$ uric acid $+ H_2O_2$	Cytoplasm in liver, small intestine, and mammary gland	(52, 109, 119, 135, 189)
NADPH oxidase	$NADPH + 2O_2 \rightarrow NADP^+ + 2O_2^{-\bullet} + H^+$	Plasma and phagosome membranes in neutrophils	(16, 73, 156)
Mitochondrial cytochrome C I,II and II	electron transport chain	Inner membrane of mitochondria	(14, 22, 60)
Monoamine oxidase	$RCH_2NH_2 + O_2 + H_2O \rightarrow RCHO + NH_3 + H_2O_2$	Outer membrane of mitochondria, plasma	(14, 22, 60, 83, 172, 199)
D-Amino acid oxidase	D-amino acids $+ O_2 + H_2O \rightarrow$ α-keto acid $+ NH_3 + H_2O_2$	Peroxisomal membranes in liver, kidney, and brain	(41, 69, 131)
Nitric oxide synthase 2, inducible (iNOS2)	L-arginine $+ 3/2$ NADPH $+$ $3/2H^+ + 2$ $O_2 \rightarrow$ L-citrulline $+$ NO $+ 3/2$ NADP$^+ + 2H_2O$	Peroxisome, plasma membrane, and cytoplasm	(89, 100, 107, 169)
[a]Fenton-type mechanism, iron redox-cycling	Fe^{2+} (ligand) $+ H_2O_2 \rightarrow Fe^{3+}$ (ligand) $+ OH^- + HO^{\bullet}$	Endoplasmic reticulum (under normal conditions)	(79, 118, 179)

[a]Nonenzymatic.
NADPH, nicotinamide adenine dinucleotide phosphate.

secrete superoxide and hydrogen peroxide to kill invading pathogens (140). The recognition of foreign particles triggers the assembly of the NADPH oxidase (NOX) complex in the phagocytic plasma membrane, which produces extracellular superoxide that is rapidly converted to hydrogen peroxide (21). After phagocytosis, the NOX complex remains on the membrane of intracellular phagocytic vesicles, producing an ROS-rich environment inside the vesicles. The fusion of phagosomes with myeloperoxidase-rich azurophilic granules in neutrophils results in the formation of hydroxyl radical and hypochlorous acid, which is pivotal in killing invading pathogens (21).

NOX1 is also expressed on the plasma membrane of non-phagocytic cells (e.g., colonic epithelium, vascular smooth muscle) and is responsible for creating an oxidative environment in the extracellular space (28). Alternately, superoxide may also react with nitric oxide (produced by NOS) and form the highly oxidizing peroxynitrite, which can, in turn, induce lipid peroxidation, causing damage to the cell membrane (28). The accumulation of extracellular hydrogen peroxide can also be attributed to its diffusion from an intracellular source (mitochondria) through the lipid bilayer or membrane-associated channels such as aquaporins (28). Cell signaling pathways at the cell surface (e.g., receptor-ligand interactions) also generate hydrogen peroxide. The production of hydrogen peroxide in response to various receptor-ligand interactions was measured in cells and was found to be enhanced when a cognate receptor-ligand pair was chosen (48). Modulators of extracellular ROS/RNS include extracellular SOD (EC-SOD), which converts superoxide anion to hydrogen peroxide, GPX3, and thioredoxin reductase (28). However, the abundance of these anti-oxidants is much lower in the extracellular space compared with the intracellular environment. Alterations in the expression of levels of NOX1 were found to be elevated in certain types of cancers, while the levels of antioxidants such as GPX3 were down-regulated in others (28).

Diseases Involving High ROS/RNS Concentrations

ROS-responsive chemistries could be used to develop diagnostics or drug carriers for any disease involving significantly increased concentrations of ROS. Here, we describe the major categories of such diseases, including the pathophysiology of several examples and how they relate to the development of ROS-responsive technologies.

Inflammatory diseases

Systemic inflammatory response syndrome. Systemic inflammatory response syndrome (SIRS), a hyperactive immune response, most commonly results from severe infection (such cases are referred to as sepsis), burns, traumatic injury, ischemia, and hemorrhage. SIRS symptoms include hyper- or hypothermia, tachycardia, hyperventilation, and leukocytosis or leukopenia (44). This aggravated systemic immune response is characterized by the release of pro-inflammatory mediators such as tumor necrosis factor alpha (TNFα), interleukin (IL)-1, IL-6, and colony-stimulating factors, which activate and recruit polymorphonuclear leukocytes (PMNs), monocytes, and macrophages (46). These cytokines also increase vascular permeability, making organs susceptible to the destructive effects of phagocytes. Recruited PMNs, especially neutrophils, generate large quantities of superoxide and hydroxyl radicals, along with hypochlorous acid in the processes of phagocytosis and degranulation as described in an earlier section (44). In addition, activated neutrophils move within tissue space by secreting extracellular matrix (ECM)-degrading enzymes (metalloproteases, collagenases, and elastases), which are the key contributors to organ failure (46). Given the high degree of neutrophil recruitment and their ability to produce huge amounts of ROS/RNS, SIRS models likely provide an excellent system to evaluate novel ROS-responsive materials.

Chronic obstructive pulmonary disease. Chronic obstructive pulmonary disease (COPD) consists of chronic bronchitis or emphysema and can progress into respiratory failure. COPD is caused by repeated exposure to oxidants in cigarette smoke and pollutants, rich in alkyl, alkoyl, and peroxyl organic-free radicals in addition to superoxide and nitric oxide, which create an oxidizing environment in the lung alveoli (53). These irritants also trigger an inflammatory response culminating in the infiltration of neutrophils and macrophages in lung tissue; viral airway infections exacerbate the disease. Patients with COPD have higher levels of neutrophils, macrophages, and CD8$^+$ cells in their peripheral airways than nonsmoking controls (126, 155). Chronic inflammation results in damage to the alveolae due to destruction of ECM by neutrophil elastase and ROS generated by activated, degranulating neutrophils (91, 137). Imbalances in lung remodeling and tissue regeneration due to increased apoptosis and autophagy of airway epithelium prevent the restoration of normal lung function (84).

If ROS concentrations are significantly enhanced, ROS-responsive materials could prove useful in the diagnosis of COPD, as the alveoli become oxidatively stressed early in disease progression and COPD is now diagnosed based on lung function, after damage has occurred.

Rheumatoid arthritis. Rheumatoid arthritis (RA) is characterized by inflammation of the synovial membrane followed by cartilage and bone damage. RA consists of an autoimmune response, usually against citrullinated vimentin and fibrinogen; environmental triggers, such as smoking, periodontitis, and exposure to microbes such as Epstein-Barr virus, cytomegalovirus, and *Escherichia coli*, are associated with enhanced citrullination of proteins (6, 106, 124, 165, 192). Autoantigen-sensitized T cells (T$_H$17 cells) and B cells in the synovium produce chemokines (IL-17 and TNFα) that recruit dendritic cells, macrophages, and granulocytes (26, 145). These leukocytes release ROS/RNS, along with cytokines, prostaglandins, and metalloproteases, inflaming the joint (25, 32). Metalloprotease activity enables synoviocyte migration out of the joint, which contributes to damage to the cartilage (114). The chemokine-rich synovial environment also promotes osteoclastic differentiation of macrophages; osteoclasts demineralize cartilage and bone (102, 176). Targeting RA therapeutics to the synovium would reduce side effects, such as the increased susceptibility to infection with TNFα inhibitors.

Atherosclerosis. Atherosclerosis is characterized by arterial lesions or plaques that are composed of cholesterol, smooth muscle cells, ECM, and leukocytes. Unstable (or vulnerable) atherosclerotic plaque is a major risk factor for sudden coronary death and it originates from the deposition of apo-B-containing lipoproteins on arterial walls (58, 195). This fatty deposition is infiltrated and phagocytosed by macrophages and dendritic cells, often giving rise to "foam cells" (103). On accumulation of excessive free cholesterol, many foam cells undergo apoptosis (159). The inability of macrophages to clear the apoptotic population from the plaque creates necrotic lesions that are susceptible to rupture (157). Furthermore, macrophages produce ROS and cytokines that are involved in the recruitment of additional leukocytes and the proliferation of smooth muscle cells into the lesion (175). ROS production has been shown to activate matrix metalloproteinases (MMPs), which promotes the destruction of the collagen matrix surrounding the plaque, further destabilizing it (148). The secretion of thrombogenic factors by macrophages on plaque rupture recruits additional platelets to form a thrombus, increasing the risk of embolism (64, 175).

Early, reliable diagnostics for vulnerable plaque would make an enormous health impact, identifying patients in need of aggressive early therapy and potentially preventing heart attacks. ROS-responsive materials may provide such a diagnostic if they are sufficiently sensitive.

Neurodegenerative diseases

The overproduction of ROS has been observed in many neurodegenerative disorders, including Parkinson's, Alzheimer's, Huntington's disease, and amyotrophic lateral sclerosis (ALS). Though these diseases cause distinct patterns of neurodegeneration (first affecting dopaminergic motor areas in Parkinson's and Huntington's, the frontal lobe in Alzheimer's, and motor neurons in ALS), similar factors, discussed next, have been shown to contribute to mitochondrial dysfunction in these diseases.

Environmental factors. The use of pesticides in developing countries has been suggested as a key risk factor for the incidence of Parkinson's disease (PD) (18). Pesticides such as

dipyridyl herbicides (paraquat), organochlorides (dieldrin), and dithiocarbamates (maneb) have been shown to interfere with the mitochondrial ETC, producing higher levels of ROS (12, 98, 203).

Mutations in genes involved in ROS regulation. Both ALS and Parkinson's have been linked to mutations in genes that regulate ROS levels, in either the cytosol or mitochondria. Many cases of familial ALS are associated with mutations in SOD1 (153), and elevated ROS and ROS-induced damage of motor neurons has been reported in postmortem ALS tissue and biopsy samples from ALS patients (8, 10). However, ALS etiology is complex and involves a combination of events, including elevated ROS, protein misfolding, endoplasmic reticulum (ER) stress, autophagosomal dysfunction, and impaired cytoskeletal rearrangement. Similarly, mutations in mitochondrial kinase PINK1, and loss of Parkin and oxidative stress sensor DJ-1 activities have been implicated in the pathogenesis of PD, with an increase in oxidative stress being one of the contributing factors for disease progression (78, 119, 146).

Inflammation. Activation of astrocytes and microglia are common to all neurodegenerative disorders. In Alzheimer's and Huntington's, insoluble protein aggregates and dying neuronal cells serve as signals for the activation and recruitment of immune cells (microglia) (72), which promote neurotoxicity by releasing additional ROS and RNS (38, 136). High ROS levels have also been observed in other protein aggregation diseases such as Alzheimer's and Huntington's disease in which the accumulation of misfolded protein aggregates has been postulated to interfere with mitochondrial function and the production of free radicals from aggregate interactions with transition metal ions such as iron, copper, and zinc (66).

Cancer

Cancer is a complex disease that is characterized by unregulated cell division of abnormal cells, which have the potential to migrate and spread to distal parts of the body. Many types of cancers are distinguished by high levels of ROS/RNS (171), which is attributed, in part, to erratic signaling and abnormal levels of cytokines and growth factors (90, 117). For example, TNFα and IFNγ signaling in certain tumors have shown to enhance levels of hydrogen peroxide and nitric oxide (117). Similarly, increased expression of oncoproteins Bcr-Abl (tyrosine kinase) (94), c-Myc, and decreased p53 activity has been correlated with increases in tumor ROS levels (184). Enhanced NOX1 expression in cancer cells has also been implicated as a major contributor to extracellular ROS; differences in NOX1 expression correlate with the degree of transformed phenotype (28).

Evidence that the overproduction of ROS/RNS contributes to the progression of cancer comes from several studies of genetically modified mice in which the expression of ROS-regulating enzymes is altered. Mouse knockouts of ROS-quenching enzymes (SOD1, SOD2, and GPX) have greater susceptibility to carcinogenesis (37, 54, 187). Transgenic mice that are deficient in SOD1 show signs of oxidative damage (lipid peroxidation and DNA damage) in the liver and develop hepatocellular carcinoma (54). The significance of ROS/RNS in cancer is further highlighted by studies demonstrating that the overexpression of EC-SOD inhibits melanoma *in vivo* and breast cancer growth *in vitro* (177, 194). Additional experiments using cancer cell lines have shown a link between ROS/RNS levels and invasiveness, presumably due to ROS/RNS-induced activation of MMPs that enable migration (28).

Detection of ROS/RNS in Biological Systems: Strategies and Challenges

Ideally, the summary cited earlier would include a comparison of ROS levels in various disease conditions; however, a reliable measurement of concentrations of these unstable species remains extremely challenging. The major challenge in measuring levels of ROS and RNS in real time is that these molecules are highly labile and therefore have a very short half life; whereas various ROS sensors have distinct sensitivities, making comparisons across studies difficult. Further, most indicators do not provide quantitative readouts. Most of the studies cited measure H_2O_2, as it is one of the most abundant and stable types of ROS. Some of the techniques to measure H_2O_2 have been reviewed here (75). Since what constitutes "biologically relevant" levels of H_2O_2 has been reviewed elsewhere (20, 80), we will focus here on tools for ROS/RNS detection; a more comprehensive list is provided in Table 2.

Chemical probes

Dichlorodihydrofluorescein diacetate. Dichlorodihydrofluorescein diacetate (H_2DCFDA) is cleaved by cellular esterases and oxidized by ROS to produce fluorescence (40, 154). H_2DCFDA and its derivatives, which freely cross cell membranes, have been widely used as ROS sensors in cell culture models (74, 116). As shown by a recent study in *Caenorhabditis elegans*, H_2DCFDA enables the study of real time *in vivo* ROS generation across tissue types; in this case, in response to challenge with *Salmonella enterica* (160). Although very popular, one of the main disadvantages of these dyes (as with other chemical probes) is that they cannot be targeted to a specific sub-cellular compartment for monitoring local changes in ROS/RNS. Moreover, they respond to a broad range of ROS/RNS and are susceptible to artifacts due to nonspecific signal amplification from photo-oxidation and reactions with heme-containing compounds (13, 141).

Amplex red. Amplex red is often used to assay mitochondrial respiration and the oxidative burst of neutrophils in suspension cultures (33, 134). Amplex red is readily oxidized to resorufin, which is highly fluorescent (134). While amplex red, unlike H_2DCFDA, is specific for H_2O_2 and can detect it at very low levels (50), it is cell impermeable and, thus, cannot be used to measure H_2O_2 levels intracellularly (50). In addition, it is susceptible to oxidation by reduced GSH and pyridine dinucleotides in the presence of NADH, creating artifacts (191).

Genetically encoded proteins

Redox-sensitive yellow and green fluorescent proteins (rxYFP and roGFP). rxYFP and roGFP were designed to noninvasively measure changes in the redox potential of cells

TABLE 2. COMMON EXAMPLES OF PROBES USED TO DETECT ROS IN CELLS OR *IN VIVO*,
INCLUDING SMALL MOLECULES, PROTEINS, AND NANOSTRUCTURES

ROS sensor	Mechanism	Sense	Readout[a]	Ref.
roGFPs	Oxidation of adjacent cysteine residues changes fluor. maximum	GRXs	Ex/Em: 400/490–510 nm	(82, 87, 130)
HyPer	Oxidization of adjacent cysteine residues changes fluor. maximum	H_2O_2	Ex/Em: 420/500–516 nm	(11, 70, 127)
Redoxfluor	Oxidation of cysteines in fragment of yeast redox sensor causes loss of FRET between cerulean and citrine	Redox potential of glutathione	Em ratio 527/476nm	(201)
DCFH-DA	Oxidation after esterase-mediated cleavage converts to fluorescent form	ROS	Ex/Em: 485/530 nm	(55)
Dihydrocalcein acetoxymethylester	Oxidation after esterase-mediated cleavage converts to fluorescent form	ROS	Ex/Em: 488/515 nm	(93, 152)
Hydroethidine (HE)	Forms a red fluorescent product that intercalates with DNA	$O_2^{-\bullet}$	Ex/Em: 518/605 nm	(19, 144, 204)
Amplex® red (10-acetyl-3,7-dihydroxyphenoxazine)	Oxidized to resorufin (colorimetric and fluorescent)	H_2O_2	Ex/Em: 563/587 nm Or Abs: 565 nm	(1, 101, 205)
FOX-2 reagent	Oxidation of iron produces a colored ferric-xylenol orange complex	H_2O_2	Abs: 560 nm	(85)
Clark's electrode	Electrochemical sensor	H_2O_2	Electrochemically	(109, 178)
Hydrocyanines	Oxidation generates extended π conjugation	$O_2^{-\bullet}$ and HO	hydro-Cy7, Ex/Em: 735/760 nm	(105)
Aryl boronic acids and esters	H_2O_2 cleaves boronate and yields fluorescent or chemiluminescent products	H_2O_2	Different generation with different Ex/Em	(43, 49, 132, 185)
Peroxalate nanoparticles containing fluorescent dyes	Oxidation of peroxalates generates high-energy dioxetanedione that excites dyes	H_2O_2	Em: 460–630 nm	(111)
Nanoreactor composed of peroxyoxalate fuel and Cy5	Oxidation of peroxyoxalate generates high-energy intermediate that excites Cy5	H_2O_2	Em: 698 nm	(115)
Hydrocyanine-conjugated, chitosan-functionalized Pluronic-based nano-carriers	Oxidation of hydrocyanine to cyanine	ROS	Ex/Em: 675/693 nm	(95)
FOSCY-1 (two linked cyanine dyes)	Oxidation of one dye releases fluorescence quenching of the other	ROS	Ex/Em: 645/668 nm and 771/813 nm	(143)

Additional examples that detect specific ROS are reviewed by Chen *et al.* (34), Lu *et al.* (120), and Freitas *et al.* (62).
[a]Wavelength may vary according to instruments.
DCF, 2′,7′-dichlorofluorescein; DCFH-DA, 2′-7′-dichlorodihydrofluorescein diacetate; GRXs, glutaredoxins; roGFPs, redox-sensitive green fluorescent proteins; ROS, reactive oxygen species.

in response to changes in environmental stimuli. To this effect, mutations were incorporated into yellow fluorescent protein to introduce a pair of redox-active cysteines that create rxYFP (142). In the oxidized state, that is, on the formation of a disulfide bond between the cysteine pair, the fluorescence of rxYFP diminishes two-fold compared with the reduced state. A similar redox variant of the green fluorescent protein (roGFP1) was also independently developed and used to characterize the reducing environment of the mitochondrial matrix in HeLa cells (82). One advantage of

TABLE 3. ARYL BORONIC ESTER-BASED OXIDATION-RESPONSIVE SYSTEMS

Polymer structure	Formulation	Oxidant	Response to oxidation	Evidence of degradation	Ref.
Modified dextran	100 nm NPs	1 mM H_2O_2	Cleavage of boronic ester yields water-soluble dextran	NMR of NP, $t_{1/2}=4$ h OD of NP, $t_{1/2}=36$ min	(17)

Modified polycresol	150 nm NPs	50, 100 μM, and 1 mM H_2O_2	Degradation into small molecules on quinone methide rearrangement	NR quenching
				  $t_{1/2} \sim 45$ h at 50 μM H_2O_2
				  $t_{1/2} \sim 30$ h at 100 μM H_2O_2
				  $t_{1/2} \sim 10$ h at 1 mM H_2O_2
				Paclitaxel release
				  63% at 50 μM H_2O_2 (3 days)
				  97% at 1 mM H_2O_2 (2 days)
				  23% (2 days) in PBS only
				NMR of polymer, complete degradation within 3 days, 50 mM H_2O_2
				TEM of NP, particle deformation within 3 days, 1 mM H_2O_2
					(45)

NPs, nanoparticles, NR, Nile red; OD, optical density; PBS, phosphate-buffered saline.

the roGFP sensors compared with rxYFP is that they can be used as ratiometric sensors of redox changes, thus minimizing measurement errors (23). However, a major disadvantage of these sensors is their slow response times, which make them unsuitable for measuring dynamic physiological changes in cells (51). To overcome this issue, the human glutaredoxin (GRX1) domain was fused onto roGFP2 and obtained GRX1-roGFP2, a more sensitive probe that enables real-time monitoring of changes in redox potentials (77). Recently, GRX1-roGFP2 and a modified roGFP (roGFP2-Orp1) were employed to monitor real-time levels of oxidized GSH and H_2O_2 in various subcellular compartments of *Drosophila*, which provided insights into changes in redox environments during development and aging (2). Recently, the development of roGFP1-iL has been reported, which enables real-time measurements of redox changes in the ER (186).

HyPer. HyPer is a genetically encoded protein that specifically detects H_2O_2 levels (11). This protein consists of a circularly permuted YFP (cpYFP) that is inserted into the regulatory domain of the *E. coli* H_2O_2-sensing protein Oxy-R (11). In response to H_2O_2, the cysteines in the Oxy-R domain of HyPer form a disulfide bond, which induces a conformational change in cpYFP that shifts its excitation maximum
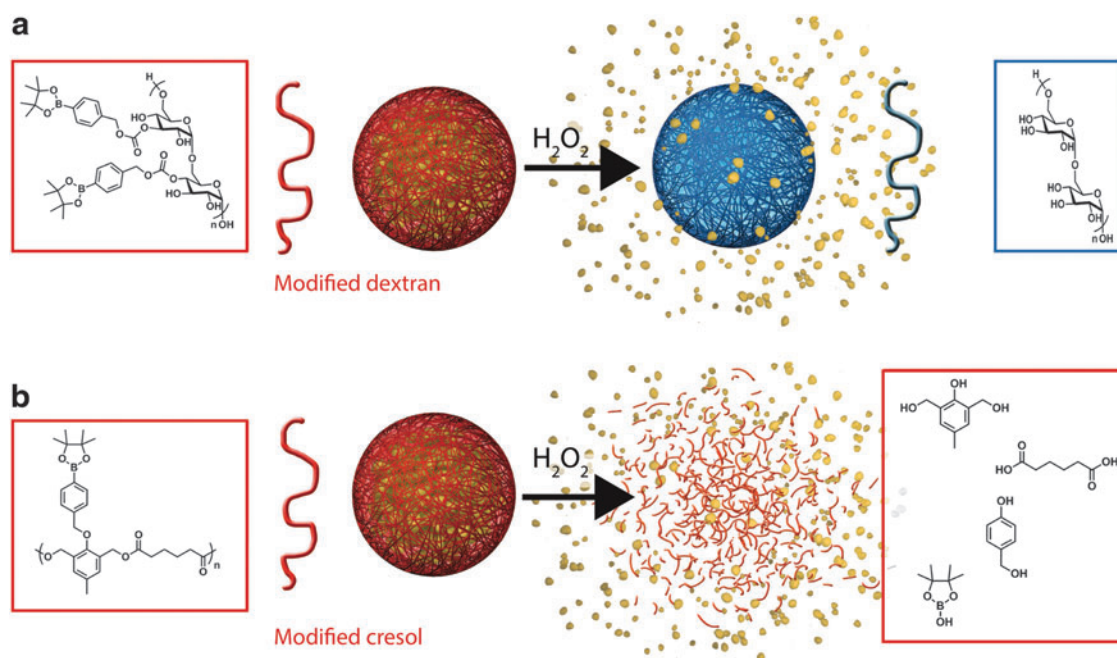

FIG. 1. **Chemical structures of aryl boronic ester-based oxidation-responsive systems and corresponding release mechanisms: modified dextran (a), modified polycresol (b)**. To see this illustration in color, the reader is referred to the web version of this article at www.liebertpub.com/ars

TABLE 4. EXAMPLES OF FERROCENE-BASED OXIDATION-RESPONSIVE SYSTEMS

Polymer structure	Formulation	Oxidant	Response to oxidation	Evidence of degradation	Ref.
Host pAA-βCD and guest pAA-Fc	Supra-molecular hydrogel	2.8 mM NaOCl	Oxidation of Fc to Fc$^+$ leads to inclusion complex dissociation and sol-gel phase transition Negligible K_a of Fc$^+$ and β-CD	Sol-gel transition	(138)
PVFc-b-PMMA	236 nm NCs with 25 nm PVFc patches, hexadecane core	1.3 M H$_2$O$_2$ or 1.1 mM KMnO$_4$	Swelling and hydration of PVFc nanopatches to create channels	Greater pyrene release in the presence of H$_2$O$_2$ than in KMnO$_4$ or no oxidant; normalized to greatest release (23 h)	(167)

-Fc, ferrocenyl group; -Fc$^+$, ferrocenium ion; K_a, association constant, β-CD, beta cyclodextrin; NCs, nanocapsules; pAA, poly(acrylic acid); pAA-β-CD, poly(acrylic acid) containing 4%–5% substitution of the COOH by βCDs; pAA-Fc, poly(acrylic acid) containing 2.7% substitution of the COOH by ferrocene groups; PVFc-b-PMMA, poly(vinylferrocene)-block-poly(methyl methacrylate).

from 420 to 500 nm (11). HyPer is a highly sensitive probe that can detect low concentrations of H$_2$O$_2$ in response to cellular signaling events (11). It can also be targeted to specific subcellular organelles for compartment-specific measurements of H$_2$O$_2$ levels (127).

Chemical probes and redox-sensing protein fluorophores suffer from inherent disadvantages as described earlier. The use of nanoparticles as redox sensors is a relatively new concept and has great potential for imaging redox changes in real time; we address this research direction in the perspectives section

Oxidation-Responsive Nanomaterials

In the previous sections, we provided an overview of the biological relevance of developing nanocarriers that are responsive to oxidative changes. Next, we describe the chemical systems developed so far that respond to altered oxidative microenvironments in the body. This description includes polymer structures and formulation, sensitivity level, response to oxidation mechanism, and degradation detection techniques. Oxidation sensitive systems reported in the literature can be classified into five categories by reactive groups: aryl boronic ester; ferrocenyl, proline oligomers, selenium, and thioether-responsive groups. Within these five categories, polymeric micellar aggregates (micelles, vesicles) or nanoparticles are the most common formulation. However, a few involve supramolecular hydrogels and terpolymer scaffolds. Typically, the response to oxidation includes swelling, dissolution, complex dissociation, decrosslinking, or degradation of the polymer matrix into small
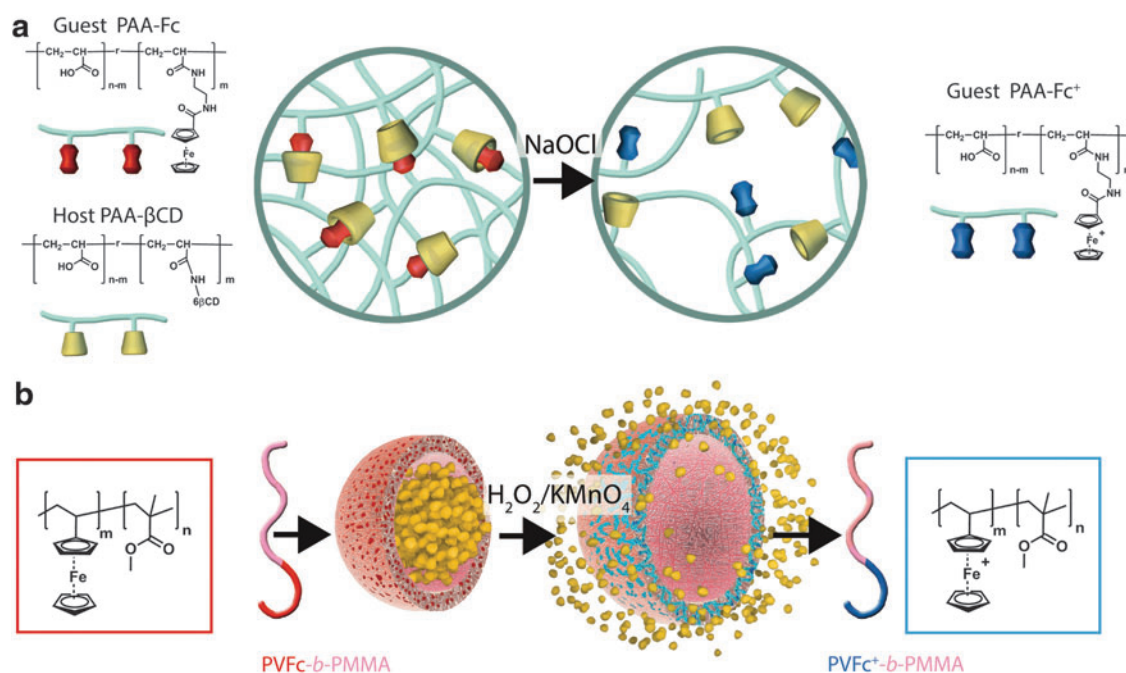

FIG. 2. **Chemical structures of ferrocene-based oxidation-responsive systems and corresponding release mechanisms: supramolecular hydrogel based on host-guest inclusion complex (a), nanocapsules containing Fc patches (b).** To see this illustration in color, the reader is referred to the web version of this article at www.liebertpub.com/ars
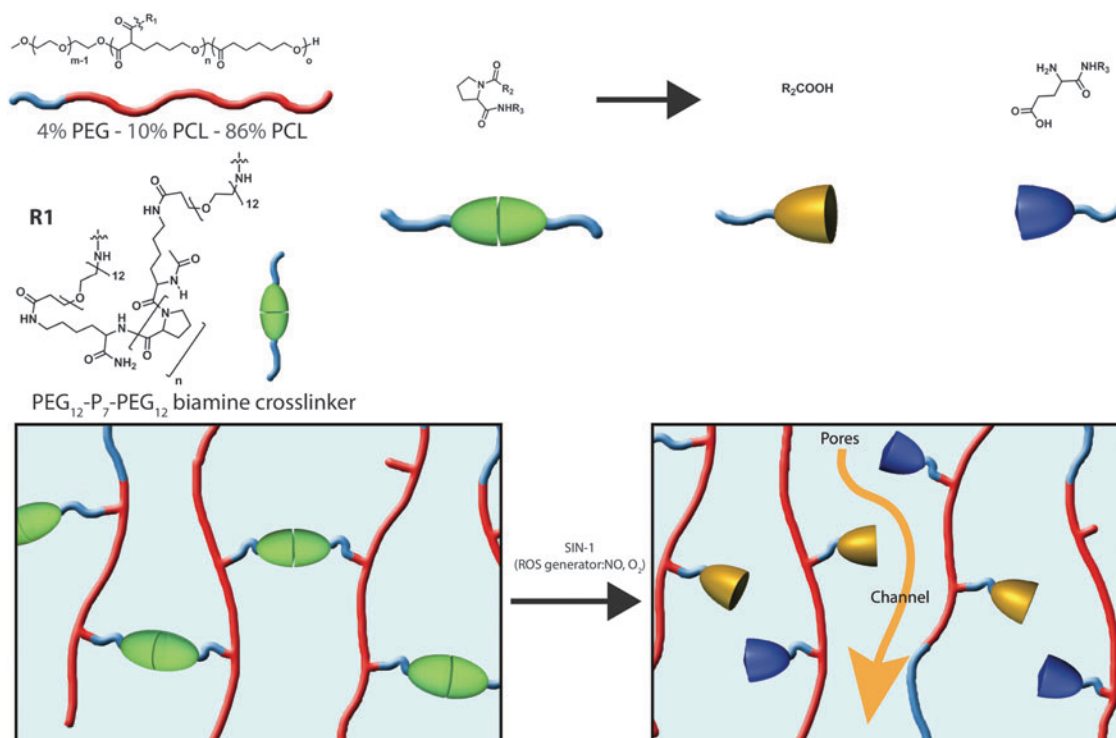
FIG. 3. **Chemical structure of proline-based oxidation-responsive system and corresponding release mechanism of a supramolecular hydrogel utilizing a PEG-oligo-proline cross-linker.** To see this illustration in color, the reader is referred to the web version of this article at www.liebertpub.com/ars

molecules, all of which would enable encapsulated cargo to diffuse out.

Chemical structures that respond to oxidation

Aryl boronic esters. Recently, probes for optical H_2O_2 imaging based on aryl boronic acid and ester deprotection chemistry, which selectively and sensitively detect physiologically relevant levels of H_2O_2, have been developed (Table 2). Inspired by this breakthrough concept, nanocarriers intended to exploit redox microenvironments as triggers for drug release *in vivo* have been introduced. On oxidation, aryl boronic ester groups are oxidized to phenols that undergo quinone methide rearrangement. These ROS-reactive groups have been incorporated into polymeric systems and yield hydrophobic dextran (17) and a cresol-based

polymer (45) (Table 3). In the presence of H_2O_2, dextran particles solubilize, as the aryl boronic groups are cleaved to leave free hydroxyl groups (Fig. 1a) and the poly-cresol degrades into small molecules (Fig. 1b); if formulated into drug-carrying particles, both processes enable drug release.

Ferrocene. The oxidation of ferrocene gives a stable cation called ferrocenium, leading to a change in polarity (hydrophobic-hydrophilic switch), as the reduced form is not charged. This hydrophobic-hydrophilic transition would either enable sol-gel transition for self-healing properties (138) or enable swelling-mediated drug release applications (167) (Table 4). Thus, host-guest inclusion complexes formed by cyclodextrins and ferrocene units are no longer stable after oxidation using chemical reagents (NaOCl) or electrochemical oxidation (Fig. 2a), and nanocapsules containing patches of ferrocene (formed

TABLE 5. PROLINE OLIGOMER (P_N)-BASED OXIDATION-RESPONSIVE SYSTEMS

Polymer structure	Formulation	Oxidant	Response to oxidation	Evidence of degradation	Ref.
4% PEG-86% PCL-10% cPCL crosslinked with PEG$_{12}$-P$_7$-PEG$_{12}$	Terpolymer scaffolds	1 mM SIN-1, which decomposes into NO and O$_2^-$ (28 days)	Creation of pores in the polymeric scaffold on oxidative cleavage of proline residues (de-crosslinking)	13.5% greater mass loss than in scaffolds cross-linked with PEG-dihydrazide DSC, ~5% lower heat capacity for melting point transition attributable to ROS-mediated hydrolysis	(202)

cPCL, poly(carboxy-ε-caprolactone); DSC, differential scanning calorimetry; percentages indicate molar proportions; PEG, poly(ethylene glycol); PCL, poly(ε-caprolactone); SIN-1, morpholinosydnonimine.
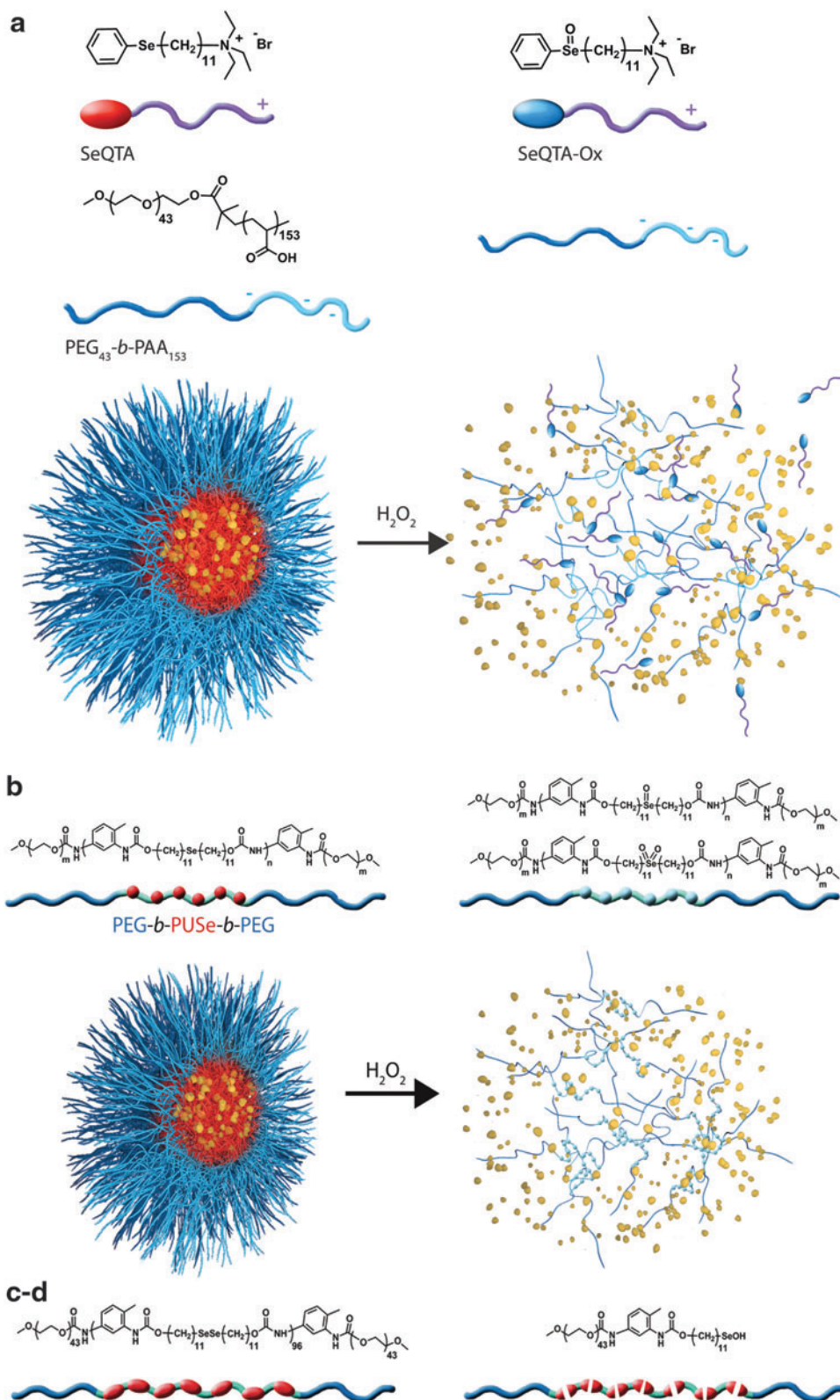
FIG. 4. **Chemical structure of selenium-based oxidation-responsive systems and corresponding release mechanisms: noncovalently connected polymeric superamphiphiles (a), main chain monoselenide and diselenide polymers (b–d), and side-chain selenium-containing polymer (e).** To see this illustration in color, the reader is referred to the web version of this article at www.liebertpub.com/ars
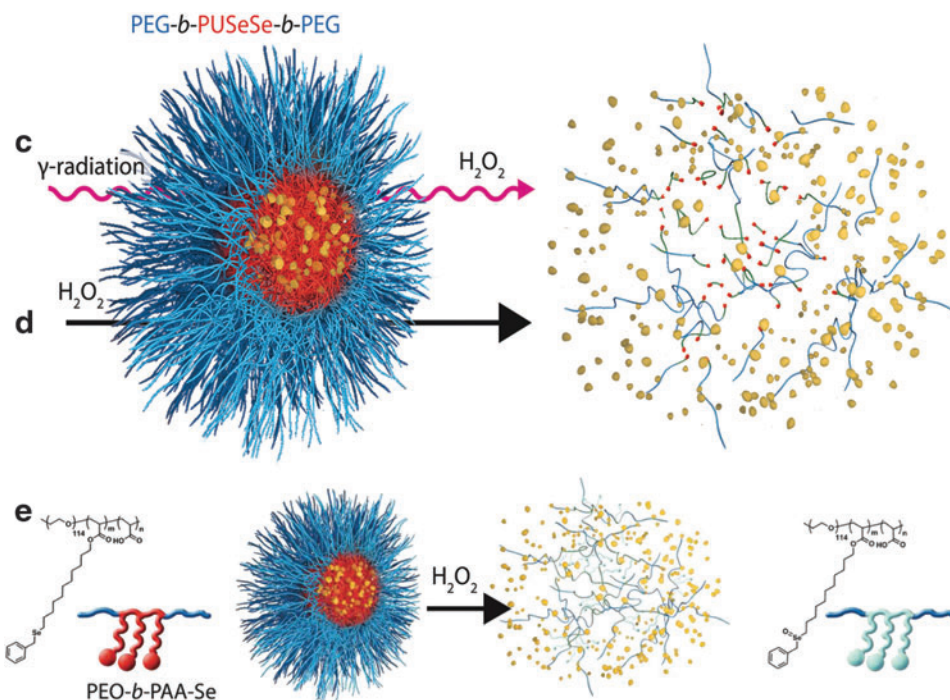
FIG. 4. (*Continued*).

spontaneously on formulation of polyvinyl ferrocene-co-poly (methyl methacrylate) release their payload on oxidation (H_2O_2, $KMnO_4$) through swollen hydrophilic channels created within the containers (Fig. 2b). Interestingly, while ferrocene itself is benign, its oxidized ferrocenium cationic analog has been shown to be toxic to tumoral cells (antiproliferative activity). Indeed, with an unpaired electron in one of the nonbonding orbitals, it becomes a stable free radical species involved in a redox-mediated toxic mechanism through hydroxyl radical formation in physiological environments (68). Other examples of ferrocene-based designs have been recently reported in the literature. They rely on electrochemical oxidation [liposome (39)], host-guest interaction-based vesicle (200), and gel (104) or chemical oxidation by large amounts of iron oxide in a micellar assembly (88). In this review, we focused on carrier designs with the potential for application in ROS-triggered drug delivery. These systems will not be a part of our classification because they do not respond to relevant biological clues.

Proline oligomers. Free amino acids and amino acids in proteins, especially histidine, proline, arginine, and lysine, are susceptible to ROS-mediated and metal-catalyzed oxidation (4, 166). On oxidative cleavage of peptide bonds, the generation of carbonyl derivatives may occur by many different mechanisms. The incorporation of proline oligomer (Pn) into poly(ethylene glycol) (PEG) cross-linkers (PEG-Pn-PEG) within a nonresponsive polymeric scaffold (Fig. 3 and Table 5) yields a system that becomes porous on oxidation-induced cleavage of the prolines, leading to gradual network hydrolysis (202).

Selenium-containing amphiphilic block copolymers. Selenium-containing amphiphilic block copolymers, including noncovalently connected polymeric superamphiphiles (81) (Fig. 4a), and polymers containing a monoselenide (121)

(Fig. 4b), diselenide in the main chain (122, 123) (Fig. 4c, d) or selenium in the side chain (150) (Fig. 4e), have also been investigated as potential ROS-responsive systems (123) (Table 6 and Fig. 4c). In each case, the amphiphilicity of the block copolymer causes self-assembly into spherical micellar aggregates. On oxidation, selenide groups are converted into selenoxide and selenone (monoselenide) or seleninic acid (R-Se-OH, in the case of diselenide bonds), which reduces amphiphilicity or cleaves the polymer, causing the aggregates to fall apart. The oxidation of selenium in side chains of amphiphilic block copolymers can also be reversed to selenide under reduction with vitamin C (150).

Thioethers. So far, thioether-based oxidation-responsive systems are the most investigated (Table 7). On oxidation, thioether moieties are converted into sulfones and sulfoxides that create highly hydrophilic molecules due to the strong dipole between oxygen and sulfur. At the molecular level, the increase in polarity and water affinity (solvation) leads to morphological disruption (76, 139) (Fig. 5a, b) or swelling and solubilization (3, 149) (Fig. 5c, d). Thioketal linkages present in all polymer subunits are completely cleaved in the presence of KO_2 (196) (Fig. 5e) or by the intracellular ROS present in cancer cells (162). Finally, in a dual-response strategy, thioether oxidation accelerates the cleavage of hydrolytically sensitive ketal groups by enabling greater solvation of the polymer (125) (Fig. 5f).

Silicon oxidation enhanced by the addition of an oxidant. Another example showed that oxidation-triggered hydrolysis of mesoporous silicon microparticles in the presence of peroxynitrite generated *in situ* by 1–2 mM morpholinosydnonimine (SIN-1) could be a potential efficient platform for ROS-triggered long-term release of covalently attached anticancer drug doxorubicin (198). However, this

TABLE 6. EXAMPLES OF SELENIUM-BASED OXIDATION-RESPONSIVE SYSTEMS

Polymer structure	Formulation	Oxidant	Response to oxidation	Evidence of degradation	Ref.
SeQTAPEG$_{43}$-b-PAA$_{153}$	Polymeric superamphi-phile micelles	0.1% H_2O_2 ($\sim$30 mM)	Disassembly of micelles after oxidation of selenide groups into hydrophilic selenoxide	TEM, micelles disappeared in 1 h Release of FluNa over $\sim$11 h, control not shown	(81)
PEG-b-PUSe-b-PEG	71 nm block copolymer aggregates	0.1% H_2O_2 ($\sim$30 mM)	Dissociation due to oxidation of selenides into hydrophilic selenoxide or selenone groups	TEM, aggregates disappear in 5 h XPS, selenoxide, and selenone formation Greater dox release (10 h) than from polysulfide analogs (72% vs. 42%)	(121)
PEG-b-PUSeSe-b-PEG	67 nm micellar aggregates	γ radiation (5 and 50 Gy)	Oxidation of diselenide groups into seleninic acid by the oxidative species (HO$^{\bullet}$, $^{\bullet}$HO$_2$, and H_2O_2) generated by water during γ-radiation Diselenide bonds cleavage induces partial disassembly and drug release	FTIR, appearance of seleninide acid TEM, swollen micelles (5 Gy) Collapsed irregular aggregates (50 Gy) Dox release in 8 h, 72% (50 Gy) 43% (5 Gy) 0% (0 Gy)	(123)
PEG-b-PUSeSe-b-PEG	76 nm micellar aggregates	0.1% H_2O_2 ($\sim$30 mM) 0.01% H_2O_2 ($\sim$3 mM)	Se-Se bonds are cleaved and oxidized to seleninic acid Diselenide bonds cleavage induces complete disassembly and drug release	NMR, appearance of seleninide acid TEM, micelle disassembly in 5 h in 0.1% H_2O_2 RB release within 5 h in 0.01 and 0.1% H_2O_2; no release in absence of H_2O_2	(122)
PEO-b-PAA-Se-64[a]	33 nm micellar aggregates	0.1% H_2O_2 ($\sim$30 mM)	Structural dissociation due to the oxidation of side-chain selenide groups into hydrophilic selenoxide groups	TEM, disassembly of the micelles in 8 h NMR and FTIR of a model compound; selenoxide appearance NR quenching within 25 h; control not shown	(150)

[a]Grafting ratio.

SeQTA, selenium-containing surfactant; XPS, X-ray photoelectron spectroscopy; FluNa, fluorescein sodium; Dox, doxorubicin, FTIR, Fourier transform infrared spectroscopy; RB, Rhodamine B.

approach requires a modification of the drug from its normal form, which might limits its application.

Formulation of oxidation-responsive materials

Heavy reliance on the formulation of ROS-sensitive polymers into micellar aggregates may inherently limit the translation of these studies into animal models. While these self-assembled amphiphilic block copolymers have several potential advantages compared with other types of nanosized drug carriers, including an excellent biocompatibility, controllable size in a range that can escape the vasculature (20–100 nm), efficient loading of hydrophobic drugs, and prolonged circulation time provided by their layer of hydrophilic antifouling shell (stealth effect) (47), these may be outweighed by their disadvantages. Specifically, after an intravenous injection, dilution causes micelles and vesicles to dissociate and aggregate, nonspecifically releasing drugs,

which decreases their targeting capability. Further, these assemblies do not efficiently penetrate tumors and are inefficiently taken up by cells due to hydrophilic surface shielding. Thus, despite the fact that polymeric micelles may enable faster release than nanoparticles on triggered destabilization, as dissociation time is faster than polymer degradation, their apparent sensitivity *in vitro* may not be a true advantage. For this reason, hydrophobic nanoparticles composed of polymers that react with ROS may be more promising candidates, offering both better physicochemical stability and more reliable tumor permeation.

Challenges in evaluating in vivo *applicability*

Unfortunately, it is difficult to compare the efficiency of release in response to ROS both across and within categories. The studies reviewed here employed varying oxidants (H_2O_2, O_2, NaOCl, KMnO$_4$, NO, and O_2^- produced by SIN-1, H_2O_2,

TABLE 7. EXAMPLES OF THIOETHER-BASED OXIDATION-RESPONSIVE SYSTEMS

Polymer structure	Formulation	Oxidant	Response to oxidation	Evidence of degradation	Ref.
EG_{16}-PS_{50}-EG_{16}	Triblock macro-amphiphiles unilamellar vesicles; membrane ~ 8 nm thick	0.03%–10% H_2O_2 (~ 9 mM-3 M)	HLB alteration and vesicle disruption due to the oxidation of the hydrophobic PPS blocks into hydrophilic polypropylene sulfoxides and sulfones	OD, clear: 10% H_2O_2 (10 h), 0.03% (300 h) TEM, vesicle number, shape change: 10% H_2O_2 (few min), 0.03% H_2O_2 (150 min) NMR, appearance of sulfoxides and sulfones	(139)
Poly(PS_{74}-b-DMA_{310})	100 nm micelles	1.1 mM-1.1 M H_2O_2, 1–100 μM $ONOO^-$, or 1–100 mM SIN-1	PPS oxidation causes micelles disassembly into unimeric polymers and cargo release	NMR, sulfone formation in H_2O_2 DLS + TEM, disruption, 1.1 M H_2O_2 NR or DiO release correlating to H_2O_2, $ONOO^-$, or SIN-1 conc.	(76)
Disulfide cross-linked PPS	25–225 nm Pluronic F127-stabilized PPS NP	5%–10% H_2O_2 (~ 1.5–3 M)	Swelling and solubilization after conversion to hydrophilic polypropylene sulfoxides and sulfones	OD, loss of turbidity: 5% H_2O_2 (30 h), 10% H_2O_2 (95 h)	(149)
PPS	150 nm Pluronic F127-stabilized PPS NP	25–200 ppm NaOCl CPO and hMPO + 200 mM NaCl, 500 μM H_2O_2	PPS oxidation causes swelling and cargo release	OD, transmittance incr. Reichardt's dye release, 98%, 5 min (2000 ppm NaOCl) NR: transmittance incr. 17%, fluor. decr. 70% (CPO); transm. incr. 10%, fluor. decr. 80% (hMPO)	(3)
PPADT	600 nm NP	KO_2 (unknown level)	Cleavage of thioketal linkages on oxidation	GPC, PPADT degradation in 8 h (high or low pH, no change)	(196)
Poly(thio-ether ketal)	200 nm NP	100 mM H_2O_2 pH: 5, 6.5, and 7.4	Dual response: thioether oxidation into sulfoxides produces more swollen and hydrophilic particles, enabling ketal hydrolysis and payload release	DLS, NP degradation, pH 5/100 mM H_2O_2, 15 h NMR, complete hydrolysis in 2 d NR quenching: >80% in 25 h, 100 mM H_2O_2 (pH 5 or pH 7); <30% in abs. OVA release: ~ 100% in 100 mM H_2O_2 (pH 6.5); <20% without H_2O_2	(125)

DLS, dynamic light scattering; EG, ethylene glycol; GPC, gel permeation chromatography; HLB, hydrophilic to lipophilic balance; hMPO, human myeloperoxidase; Mn, number average molecular weight; OD, optical density; PPS, poly(propylene sulfide); PS, propylene sulfide; PGSE, pulse gradient spin echo; PPADT, poly-(1,4-phenyleneacetone dimethylene thioketal); poly(PS_{74}-b-DMA_{310}), a diblock polymer of propylene sulfide (PS) and N,N-dimethylacrylamide; DiO, (3,3′-dioctadecyloxacarbocyanine perchlorate); CPO, chloroperoxidase; OVA, ovalbumin Alexa Fluor 594; NMR, nuclear magnetic resonance.
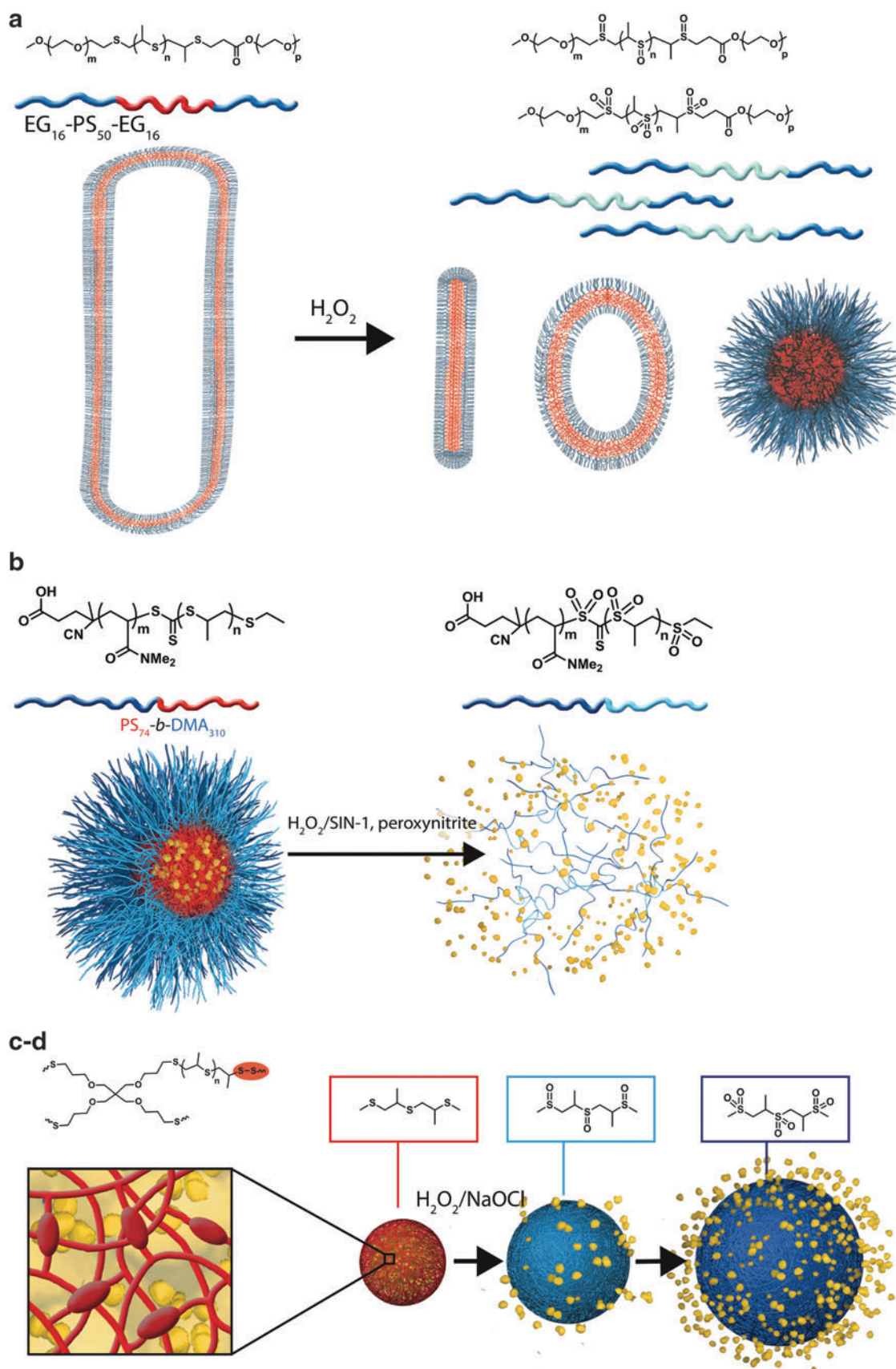
FIG. 5. Chemical structure of thioether-based oxidation-responsive systems and corresponding release mechanisms: thioether (a–d), thioketal (e), and thioether-ketal (f). To see this illustration in color, the reader is referred to the web version of this article at www.liebertpub.com/ars
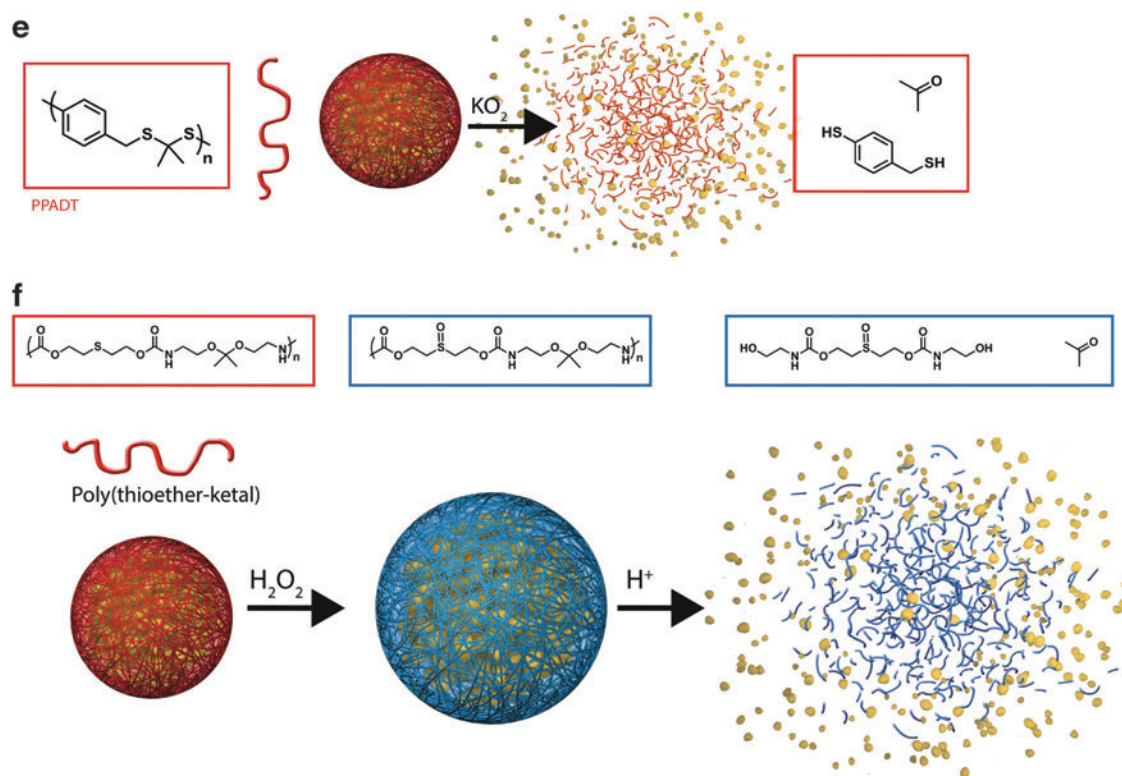
FIG. 5. (*Continued*).

and radicals generated by γ-radiation, KO$_2$), concentrations of ROS (for H$_2$O$_2$, from 50–100 μM to concentrations as high as 3 M), and ratios between the responsive polymer assembly and oxidative agent. While some papers claim that 0.1% ($\sim$30 mM) H$_2$O$_2$ is a quite mild oxidative environment, this level is far from the biologically relevant range (50–100 μM) (80). However, even polymeric assemblies that release cargo only in response to high concentrations of H$_2$O$_2$ *in vitro* may be sensitive enough, given that H$_2$O$_2$ is converted to hydroxyl radical in the body spontaneously on an interaction with transition metal ions, such as iron, and hydroxyl radical is more reactive than H$_2$O$_2$. Another important consideration is that oxidizing agents can affect pH, so the apparent ROS sensitivity of chemical structures that degrade or change hydrophilicity in response to pH may be inaccurate. Molar concentrations of H$_2$O$_2$ in water can cause the pH to be acidic, while molar concentrations of NaOCl can shift it above 9.

Moreover, within the same study, different detection methods yield different results (transmission electron microscopy (TEM), payload release, nuclear magnetic resonance spectroscopy, and light scattering), which further limits any comparison. More precisely, detection methods vary in their sensitivity; for example, turbidity measurements are far less sensitive than fluorescence, and Nile red quenching may or may not correlate with degradation, as water diffusion into the hydrophobic core would also cause quenching. Calculating payload release relative to the total amount encapsulated and not only as a function of time would give an evaluation of release that could more easily be compared across various nanocarrier assemblies and cargos.

Thus, additional measures of nanocarrier degradation such as TEM or real quantification of drugs by liquid chromatography-mass spectroscopy should become standard within the field. Indirect methods using light scattering or transmission do not provide as detailed an understanding of the mechanism by which particles degrade as does TEM imaging. On degradation, nanoparticle polydispersity increases, and the refractive index and viscosity of the solution change. Since dynamic light scattering calculations assume constant refractive index and viscosity values, these readings can be unreliable. Further, TEM enables a more detailed understanding of how particles degrade and release cargo, as changes in morphology can be directly visualized. For instance, our group used TEM to detail significant changes in nanoparticle morphology after treatment with H$_2$O$_2$, such as ripping or crumpling of the structures, as well as particle expansion (45).

A few direct comparisons of polymeric carriers' sensitivity to oxidative agents have been made. Only one study has compared the sensitivity of polyselenide block copolymer-based micellar aggregates with polysulfide analogues and reports that selenide moieties are more sensitive: The lower binding energy of Se-C bond compared with S-C bond makes Se-containing molecules more sensitive to oxidative stimuli (121).

The design of some systems to respond to a combination of acidic pH with oxidative conditions (125) may enhance their usefulness in specific disease conditions. Since the pH in tumors and inflamed tissues is known to be slightly acidic, nanoparticles that degrade specifically in response to both stimuli may better target drug delivery to those conditions.

In diselenide cross-linked polymeric carriers (122), the linkages are also cleaved by a reduction in the presence of thiols. For example, in the dual-responsive assemblies
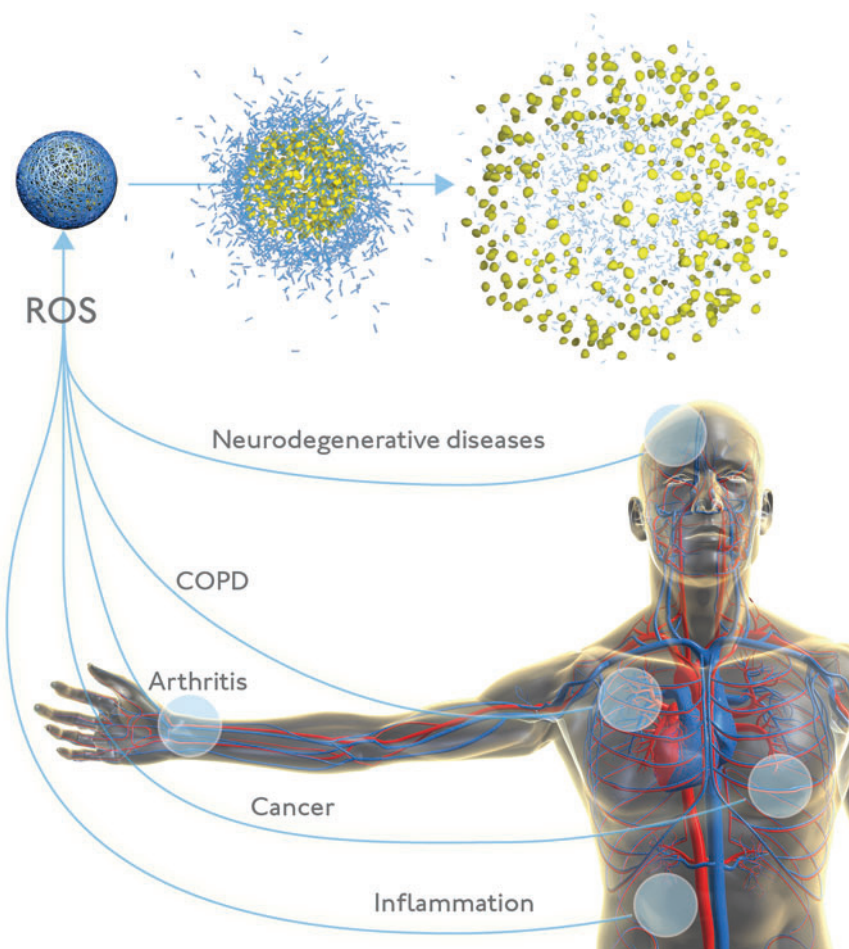
FIG. 6. Reactive oxygen species-responsive nanocarriers that release payload in response to redox changes in the microenvironment have tremendous potential as diagnostic and therapeutic agents for a variety of pathophysiological conditions. To see this illustration in color, the reader is referred to the web version of this article at www.liebertpub.com/ars

(diselenide block copolymers), *in vitro* release was demonstrated in the presence of both oxidizing (H_2O_2) and reducing agents (GSH) (122). Since the cytosol of healthy cells has a strong reducing environment, such particles could release cargo through the reducing mechanism if endocytosed. However, the intracellular accumulation of polymeric nanoparticles by nonendothelial cells is uncommon; significant uptake generally requires that particles be decorated with targeting moieties or cell-penetrating peptides [reviewed in (206)]. Circulating nontargeted particles are more likely to be either phagocytosed or encounter an extracellular environment that is oxidative (especially in the diseases described earlier), triggering release.

Biologically relevant ROS-responsive systems. This review highlights various chemistries that can be used to formulate drug carriers which are sensitive to oxidation. In most studies developing novel ROS-sensitive nanocarriers, the assessment of payload release is performed *in vitro* using concentrations of oxidants that are several fold higher than biologically relevant levels. While a huge challenge in testing oxidation-responsive carriers is the extremely short half life of these oxidant molecules (ROS/RNS), model cell culture systems can be considered useful tools for providing insights into the sensitivity of such nanocarriers. For example, macrophage (*e.g.*, Raw264.7) and neutrophil (*e.g.*, mouse promyelocyte) cell lines can be manipulated to produce an oxidative burst.

Studies in activated macrophages and neutrophils have demonstrated that several systems, including a boronic ester-modified polymeric particle (45), a polymer-based hydrogel cross-linked with proline oligomers (202), and micelles composed of a poly(propylene sulfide) (PPS) core (76), respond to biological levels of H_2O_2. The first of these studies was especially well controlled, as it compared responsiveness of the designed ROS-sensitive polymer with that of poly(lactic-*co*-glycolic) acid (PLGA) and a control polymer lacking ROS-reactive groups; neither control releases cargo in response to activated neutrophils (45). This finding may lead to the polymer's use in targeting drugs to tissues that are characterized by a high level of neutrophils (*e.g.*, inflammatory diseases such as SIRS and COPD). Though the PPS micelle study only demonstrated a 10% difference between release induced by activated and nonactivated macrophages, their release assay was creative: a reduction in fluorescence resonance energy transfer between co-encapsulated dyes (76). Systems such as this that were demonstrated to respond to activated macrophages could prove useful for targeting drugs to sites which are rich in these cells, such as vulnerable atherosclerotic plaques. Since ROS-responsive systems may prove useful for the delivery of vaccine formulations, one group has tested their ability to enhance CD8^{+} presentation by T cells on uptake by dendritic cells *in vitro*. Broaders *et al.* showed that their aryl boronic ester-modified dextran particles produced a 27-fold greater enhancement of CD8^{+} presentation than ovalbumin in PLGA (17). Another interesting application of ROS-responsive polymers is for gene delivery to cancer cells with high ROS/RNS. ROS/RNS-sensitive

poly(amino thioketal) was shown to have a higher efficiency of gene delivery and expression compared with non-degradable poly-amine or the commonly used transfection agent (branched polyethyleneimine) (162). In addition, the authors conjugated a GRP78 binding peptide to the polymer to further enhance uptake by cancer cells.

The only *in vivo* investigation on oxidation-responsive nanoparticles to date shows the advantage of anti-inflammatory agents in oxidation-sensitive particles compared with a slowly degrading material, PLGA, for oral delivery. In a murine model of ulcerative colitis induced by the administration of dextran sodium sulfate in drinking water (196), TNFα-siRNA complexed with DOTAP (cationic lipid, 1,2-dioleoyl-3-trimethyl-lammonium-propane) encapsulated into thioketal particles (TNFα-TKNs) induced a ten-fold decrease in TNFα-mRNA expression in the colon; while TNFα-siRNA in PLGA had no significant effect. This superiority of thioketal particles was likely due to the combined effect of the stability of TKNs against the harsh gastric environment and their ability to degrade in response to ROS produced by inflamed intestinal tissue.

Though only one ROS-responsive system has been tested *in vivo*, others have demonstrated the utility of nanoparticles for delivering reactive antioxidants. For example, a novel redox nanoparticle (RNP^O) consisting of a self-assembling ampiphilic block copolymer containing a derivative of the antioxidant TEMPOL (4-hydroxy-2,2,6,6-tetramethylpiperidin-1-oxyl) in the hydrophobic segment has been shown to be more effective than free TEMPOL or mesalamine (an anti-inflammatory compound) at treating colitis in mice (190).The confinement of the nitroxide radical-containing TEMPOL derivative in the hydrophobic core of RNP^O nanoparticles enhanced its biocompatibility, and the nanoparticles' size (40 nm) caused them to accumulate in the colonic mucosa. A recent report described the antioxidant properties of nanoparticles (PVAX) formulated from copolyoxylate containing vanillyl alcohol (VA) (110). The PVAX polymer consists of peroxalate ester bonds along with VA in the backbone. Under physiological conditions PVAX is hydrolytically cleaved and releases VA, which has therapeutic effects (anti-inflammatory, antioxidant, and anti-cociceptive) (110). In addition, the PVAX nanoparticles were shown to scavenge hydrogen peroxide in a concentration-dependent manner. Finally, the authors demonstrated the therapeutic efficacy of these nanoparticles in an ischemia/repurfusion model in mice (110). These examples further illustrate that nanoparticles can be designed as therapeutics rather than simply as carriers.

Perspectives

The future of these ROS/RNS-responsive carriers depends on whether they are truly sensitive to the levels of ROS/RNS produced in disease conditions. Given the scarcity of studies that have examined this directly, predicting which chemistries will prove most useful remains impossible. Thus, extensive further studies are needed for examining the effectiveness of those ROS/RNS-responsive chemistries that prove sensitive to biologically produced ROS/RNS in cell culture systems. These studies should be judicious in their choice of disease model, as each system likely has varying sensitivity to ROS, and dosing route, as nontargeted particles may not accumulate in intended tissues if administered systemically. Further, while the exact ROS levels and species in various disease models remain unknown (see section on Detection of ROS/RNS in biological

systems), the variety of mechanisms of ROS/RNS production suggests that some disease states likely involve much higher levels than others. The disease models described thus far to test redox-responsive nanoparticles rely on the production of an aggravated immune response (*e.g.*, dextran sodium sulfate-induced colitis), which likely produces a tremendous amount of ROS/RNS due to oxidative burst from accumulated phagocytes. While such a model has direct applicability in terms of human disease (ulcerative colitis), it would be interesting to determine whether some ROS/RNS-responsive carriers respond as well to oxidative stress produced in other conditions (*e.g.*, cancer).

An especially exciting potential application of oxidation-responsive nanoparticles would be to directly assess the question of ROS levels in various disease states (Fig. 6), filling in the unknown that currently limits the assessment of *in vivo* applicability. The applicability of existing chemical ROS probes is largely restricted to cell culture, as they have poor retention in animal models. Genetically encoded proteins, on the other hand, need to be stably incorporated into the genome or transfected into the tissue being studied. While these protein ROS sensors are useful tools for cell and animal research, sensors that enable the measurement of ROS in humans would be even more useful. ROS-responsive nanoparticles may represent this translatable technology, as they are generally biocompatible, circulate for extended periods, and may be targeted to specific tissues.

There is a growing body of literature on nanoparticle-based ROS/RNS sensors that incorporate various imaging modalities (fluorescence, luminescence, Raman scattering, *etc.*) to detect redox changes, and some of these have been used to image ROS/RNS *in vivo* in tumors [reviewed in detail elsewhere (183)]. Those applied *in vivo* have so far been limited to chemiluminescent sensors, which detect the ROS produced in response to lipopolysaccharide-induced inflammation (111, 115). However, neither of these studies attempted to quantify ROS levels, suggesting that chemiluminescence does not correlate with ROS concentration. Thus, nanosystems that provide concentration-dependent signals may be more promising for this purpose; sensors based on the quenching of metallic nanoparticle fluorescence show such a response *in vitro*. For example, CdSe/ZnS quantum dots conjugated to oxidized cytochrome c; oxidation by $O_2^{\bullet-}$ enhances fluorescence (113). Further along these lines, oxidation-responsive nanoparticles could also be employed to develop an ROS-detecting magnetic resonance imaging contrast system *via* release of Gd-based contrast agents from hydrophobic assemblies and resulting in de-quenching of contrast enhancement (188). In summary, the oxidation-sensitive chemistries described here offer exciting new prospects in the field of nanomedicine, specifically targeting microenvironments with perturbations in redox levels.

Acknowledgments

References

1. Ahmed H. *Principles and Reactions of Protein Extraction, Purification, and Characterization*. Boca Raton, FL: Taylor & Francis, 2004.

2. Albrecht SC, Barata AG, Grosshans J, Teleman AA, and Dick TP. *In vivo* mapping of hydrogen peroxide and oxidized glutathione reveals chemical and regional specificity of redox homeostasis. *Cell Metab* 14: 819–829, 2011.

3. Allen BL, Johnson JD, and Walker JP. Encapsulation and enzyme-mediated release of molecular cargo in polysulfide nanoparticles. *ACS Nano* 5: 5263–5272, 2011.

4. Amici A, Levine RL, Tsai L, and Stadtman ER. Conversion of amino-acid residues in proteins and amino-acid homopolymers to carbonyl derivatives by metal-catalyzed oxidation reactions. *J Biol Chem* 264: 3341–3346, 1989.

5. Antonenkov VD, Grunau S, Ohlmeier S, and Hiltunen JK. Peroxisomes are oxidative organelles. *Antioxid Redox Signal* 13: 525–537, 2010.

6. Auger I and Roudier J. A function for the QKRAA amino acid motif: mediating binding of DnaJ to DnaK. Implications for the association of rheumatoid arthritis with HLA-DR4. *J Clin Invest* 99: 1818–1822, 1997.

7. Avissar N, Slemmon JR, Palmer IS, and Cohen HJ. Partial sequence of human plasma glutathione peroxidase and immunologic identification of milk glutathione peroxidase as the plasma enzyme. *J Nutrition* 121: 1243–1249, 1991.

8. Barber SC and Shaw PJ. Oxidative stress in ALS: key role in motor neuron injury and therapeutic target. *Free Radic Biol Med* 48: 629–641, 2010.

9. Barrera G, Pizzimenti S, and Dianzani MU. Lipid peroxidation: control of cell proliferation, cell differentiation and cell death. *Mol Aspects Med* 29: 1–8, 2008.

10. Beal MF, Ferrante RJ, Browne SE, Matthews RT, Kowall NW, Brown RH, Jr. Increased 3-nitrotyrosine in both sporadic and familial amyotrophic lateral sclerosis. *Ann Neurol* 42: 644–654, 1997.

11. Belousov VV, Fradkov AF, Lukyanov KA, Staroverov DB, Shakhbazov KS, Terskikh AV, and Lukyanov S. Genetically encoded fluorescent indicator for intracellular hydrogen peroxide. *Nat Methods* 3: 281–286, 2006.

12. Berisha HI, Pakbaz H, Absood A, and Said SI. Nitric oxide as a mediator of oxidant lung injury due to paraquat. *Proc Natl Acad Sci U S A* 91: 7445–7449, 1994.

13. Bilski P, Belanger AG, and Chignell CF. Photosensitized oxidation of 2',7'-dichlorofluorescin: singlet oxygen does not contribute to the formation of fluorescent oxidation product 2′,7′-dichlorofluorescein. *Free Radic Biol Med* 33: 938–946, 2002.

14. Boveris A. Determination of the production of superoxide radicals and hydrogen-peroxide in mitochondria. *Meth Enzymol* 105: 429–435, 1984.

15. Boveris A and Chance B. The mitochondrial generation of hydrogen peroxide. General properties and effect of hyperbaric oxygen. *Biochem J* 134: 707–716, 1973.

16. Briggs RT, Drath DB, Karnovsky ML, and Karnovsky MJ. Localization of NADH oxidase on the surface of human polymorphonuclear leukocytes by a new cytochemical method. *J Cell Biol* 67: 566–586, 1975.

17. Broaders KE, Grandhe S, and Frechet JMJ. A Biocompatible Oxidation-Triggered Carrier Polymer with Potential in Therapeutics. *J Am Chem Soc* 133: 756–758, 2011.

18. Brown TP, Rumsby PC, Capleton AC, Rushton L, and Levy LS. Pesticides and Parkinson's disease—is there a link? *Environ Health Perspect* 114: 156–164, 2006.

19. Budd SL, Castilho RF, and Nicholls DG. Mitochondrial membrane potential and hydroethidine-monitored superoxide generation in cultured cerebellar granule cells. *FEBS Lett* 415: 21–24, 1997.

20. Burgoyne JR, Oka S, Ale-Agha N, and Eaton P. Hydrogen peroxide sensing and signaling by protein kinases in the cardiovascular system. *Antioxid Redox Signal* 18: 1042–1052, 2013.

21. Bylund J, Brown KL, Movitz C, Dahlgren C, and Karlsson A. Intracellular generation of superoxide by the phagocyte NADPH oxidase: how, where, and what for? *Free Radic Biol Med* 49: 1834–1845, 2010.

22. Cadenas E and Davies KJA. Mitochondrial free radical generation, oxidative stress, and aging. *Free Radic Biol Med* 29: 222–230, 2000.

23. Cannon MB and Remington SJ. Redox-sensitive green fluorescent protein: probes for dynamic intracellular redox responses. A review. *Methods Mol Biol* 476: 51–65, 2008.

24. Castegna A, Aksenov M, Aksenova M, Thongboonkerd V, Klein JB, Pierce WM, Booze R, Markesbery WR, and Butterfield DA. Proteomic identification of oxidatively modified proteins in Alzheimer's disease brain. Part I: creatine kinase BB, glutamine synthase, and ubiquitin carboxy-terminal hydrolase L-1. *Free Radic Biol Med* 33: 562–571, 2002.

25. Cedergren J, Forslund T, Sundqvist T, and Skogh T. Intracellular oxidative activation in synovial fluid neutrophils from patients with rheumatoid arthritis but not from other arthritis patients. *J Rheumatol* 34: 2162–2170, 2007.

26. Chabaud M, Aarvak T, Garnero P, Natvig JB, and Miossec P. Potential contribution of IL-17-producing Th(1)cells to defective repair activity in joint inflammation: partial correction with Th(2)-promoting conditions. *Cytokine* 13: 113–118, 2001.

27. Chae HZ, Chung SJ, and Rhee SG. Thioredoxin-dependent peroxide reductase from yeast. *J Biol Chem* 269: 27670–27678, 1994.

28. Chaiswing L and Oberley TD. Extracellular/microenvironmental redox state. *Antioxid Redox Signal* 13: 449–465, 2010.

29. Chance B, Sies H, and Boveris A. Hydroperoxide metabolism in mammalian organs. *Physiol Rev* 59: 527–605, 1979.

30. Chang CH, Schiller B, and Goldfischer S. Small cytoplasmic bodies in the loop of Henle and distal convoluted tubule that resemble peroxisomes. *J Histochem Cytochem* 19: 56–62, 1971.

31. Chang LY, Slot JW, Geuze HJ, and Crapo JD. Molecular immunocytochemistry of the cuzn superoxide-dismutase in rat hepatocytes. *J Cell Biol* 107: 2169–2179, 1988.

32. Chatham WW, Swaim R, Frohsin H, Jr., Heck LW, Miller EJ, and Blackburn WD, Jr. Degradation of human articular cartilage by neutrophils in synovial fluid. *Arthritis Rheum* 36: 51–58, 1993.

33. Chen Q, Vazquez EJ, Moghaddas S, Hoppel CL, and Lesnefsky EJ. Production of reactive oxygen species by mitochondria: central role of complex III. *J Biol Chem* 278: 36027–36031, 2003.

34. Chen XQ, Tian XZ, Shin I, and Yoon J. Fluorescent and luminescent probes for detection of reactive oxygen and nitrogen species. *Chem Soc Rev* 40: 4783–4804, 2011.

35. Chu F, Esworthy R, Doroshow J, Doan K, and Liu X. Expression of plasma glutathione peroxidase in human liver in addition to kidney, heart, lung, and breast in humans and rodents. *Blood* 79: 3233–3238, 1992.

36. Chu FF, Doroshow JH, and Esworthy RS. Expression, characterization, and tissue distribution of a new cellular selenium-dependent glutathione peroxidase, GSHPx-GI. *J Biol Chem* 268: 2571–2576, 1993.

37. Chu FF, Esworthy RS, Chu PG, Longmate JA, Huycke MM, Wilczynski S, and Doroshow JH. Bacteria-induced intestinal cancer in mice with disrupted Gpx1 and Gpx2 genes. *Cancer Res* 64: 962–968, 2004.

38. Colton CA, Yao JB, Gilbert D, and Oster-Granite ML. Enhanced production of superoxide anion by microglia from trisomy 16 mice. *Brain Res* 519: 236–242, 1990.

39. Correia-Ledo D, Arnold AA, and Mauzeroll J. Synthesis of redox active ferrocene-modified phospholipids by transphosphatidylation reaction and chronoamperometry study of the corresponding redox sensitive liposome. *J Am Chem Soc* 132: 15120–15123, 2010.

40. Crow JP. Dichlorodihydrofluorescein and dihydrorhodamine 123 are sensitive indicators of peroxynitrite *in vitro*: implications for intracellular measurement of reactive nitrogen and oxygen species. *Nitric Oxide* 1: 145–157, 1997.

41. D'Aniello A, D'Onofrio G, Pischetola M, D'Aniello G, Vetere A, Petrucelli L, and Fisher GH. Biological role of D-amino acid oxidase and D-aspartate oxidase. Effects of D-amino acids. *J Biol Chem* 268: 26941–26949, 1993.

42. D'Autreaux B and Toledano MB. ROS as signalling molecules: mechanisms that generate specificity in ROS homeostasis. *Nat Rev Mol Cell Biol* 8: 813–824, 2007.

43. Daniel KB, Agrawal A, Manchester M, and Cohen SM. Readily accessible fluorescent probes for sensitive biological imaging of hydrogen peroxide. *Chembiochem* 14: 593–598, 2013.

44. Davies MG and Hagen PO. Systemic inflammatory response syndrome. *Br J Surg* 84: 920–935, 1997.

45. de Gracia Lux C, Joshi-Barr S, Nguyen T, Mahmoud E, Schopf E, Fomina N, and Almutairi A. Biocompatible polymeric nanoparticles degrade and release cargo in response to biologically relevant levels of hydrogen peroxide. *J Am Chem Soc* 134: 15758–15764, 2012.

46. de Jong HK, van der Poll T, and Wiersinga WJ. The systemic pro-inflammatory response in sepsis. *J Innate Immun* 2: 422–430, 2010.

47. Deng C, Jiang YJ, Cheng R, Meng FH, and Zhong ZY. Biodegradable polymeric micelles for targeted and controlled anticancer drug delivery: promises, progress and prospects. *Nano Today* 7: 467–480, 2012.

48. DeYulia GJ, Jr., Carcamo JM, Borquez-Ojeda O, Shelton CC, and Golde DW. Hydrogen peroxide generated extracellularly by receptor-ligand interaction facilitates cell signaling. *Proc Natl Acad Sci U S A* 102: 5044–5049, 2005.

49. Dickinson BC, Huynh C, and Chang CJ. A palette of fluorescent probes with varying emission colors for imaging hydrogen peroxide signaling in living cells. *J Am Chem Soc* 132: 5906–5915, 2010.

50. Dikalov S, Griendling KK, and Harrison DG. Measurement of reactive oxygen species in cardiovascular studies. *Hypertension* 49: 717–727, 2007.

51. Dooley CT, Dore TM, Hanson GT, Jackson WC, Remington SJ, and Tsien RY. Imaging dynamic redox changes in mammalian cells with green fluorescent protein indicators. *J Biol Chem* 279: 22284–22293, 2004.

52. ED J, C G, G B, HW H, TW K, and WW F. Localization of xanthine oxidase in mammary-gland epithelium and capillary. *Cell* 25: 67–82, 1981.

53. Eiserich JP, van der Vliet A, Handelman GJ, Halliwell B, and Cross CE. Dietary antioxidants and cigarette smoke-induced biomolecular damage: a complex interaction. *Am J Clin Nutr* 62: 1490S–1500S, 1995.

54. Elchuri S, Oberley TD, Qi W, Eisenstein RS, Jackson Roberts L, Van Remmen H, Epstein CJ, and Huang TT. CuZnSOD deficiency leads to persistent and widespread oxidative damage and hepatocarcinogenesis later in life. *Oncogene* 24: 367–380, 2005.

55. Eruslanov E and Kusmartsev S. Identification of ROS using oxidized DCFDA and flow-cytometry. In: *T Advanced Protocols in Oxidative Stress II*. 2009, pp. 57–72.

56. Esworthy RS, Ho YS, and Chu FF. The Gpx1 gene encodes mitochondrial glutathione peroxidase in the mouse liver. *Arch Biochem Biophys* 340: 59–63, 1997.

57. Finkel T. Signal transduction by reactive oxygen species. *J Cell Biol* 194: 7–15, 2011.

58. Finn AV, Nakano M, Narula J, Kolodgie FD, and Virmani R. Concept of vulnerable/unstable plaque. *Arterioscler Thromb Vasc Biol* 30: 1282–1292, 2010.

59. Finocchietto PV, Franco MC, Holod S, Gonzalez AS, Converso DP, Antico Arciuch VG, Serra MP, Poderoso JJ, and Carreras MC. Mitochondrial nitric oxide synthase: a masterpiece of metabolic adaptation, cell growth, transformation, and death. *Exp Biol Med (Maywood)* 234: 1020–1028, 2009.

60. Forman HJ and Boveris A. Chapter 3- Superoxide radical and hydrogen peroxide in mitochondria. In: *Free Radicals in Biology*, edited by William Pryor. London: Academic Press, 1982, pp. 65–90.

61. Fransen M, Nordgren M, Wang B, and Apanasets O. Role of peroxisomes in ROS/RNS-metabolism: implications for human disease. *Biochim Biophys Acta* 1822: 1363–1373, 2012.

62. Freitas M, Lima JLFC, and Fernandes E. Optical probes for detection and quantification of neutrophils' oxidative burst. A review. *Analyt Chim Acta* 649: 8–23, 2009.

63. Fridovich I. Superoxide dismutases. *Ann Rev Biochem* 44: 147–159, 1975.

64. Friedman M and Van den Bovenkamp GJ. The pathogenesis of a coronary thrombus. *Am J Pathol* 48: 19–44, 1966.

65. Fukai T, Folz RJ, Landmesser U, and Harrison DG. Extracellular superoxide dismutase and cardiovascular disease. *Cardiovasc Res* 55: 239–249, 2002.

66. Gaeta A and Hider RC. The crucial role of metal ions in neurodegeneration: the basis for a promising therapeutic strategy. *Br J Pharmacol* 146: 1041–1059, 2005.

67. Gaetani GF, Galiano S, Canepa L, Ferraris AM, and Kirkman HN. Catalase and glutathione peroxidase are equally active in detoxification of hydrogen peroxide in human erythrocytes. *Blood* 73: 334–339, 1989.

68. Gasser G, Ott I, and Metzler-Nolte N. Organometallic anticancer compounds. *J Med Chem* 54: 3–25, 2011.

69. Gaunt GL and Deduve C. Subcellular-distribution of D-amino-acid oxidase and catalase in rat-brain. *J Neurochem* 26: 749, 1976.

70. Gehrmann W and Elsner M. A specific fluorescence probe for hydrogen peroxide detection in peroxisomes. *Free Rad Res* 45: 501–506, 2011.

71. Giulivi C, Boveris A, and Cadenas E. Hydroxyl radical generation during mitochondrial electron transfer and the formation of 8-hydroxydesoxyguanosine in mitochondrial DNA. *Arch Biochem Biophys* 316: 909–916, 1995.

72. Glass CK, Saijo K, Winner B, Marchetto MC, and Gage FH. Mechanisms underlying inflammation in neurodegeneration. *Cell* 140: 918–934, 2010.

73. Goldstein IM, Cerqueira M, Lind S, and Kaplan HB. Evidence that the superoxide-generating system of human

leukocytes is associated with the cell surface. *J Clin Invest* 59: 249–254, 1977.

74. Graves JA, Metukuri M, Scott D, Rothermund K, and Prochownik EV. Regulation of reactive oxygen species homeostasis by peroxiredoxins and c-Myc. *J Biol Chem* 284: 6520–6529, 2009.

75. Grisham MB. Methods to detect hydrogen peroxide in living cells: possibilities and pitfalls. *Comp Biochem Physiol A Mol Integr Physiol* 165: 429–438, 2013.

76. Gupta MK, Meyer TA, Nelson CE, and Duvall CL. Poly(PS-b-DMA) micelles for reactive oxygen species triggered drug release. *J Controlled Release* 162: 591–598, 2012.

77. Gutscher M, Pauleau AL, Marty L, Brach T, Wabnitz GH, Samstag Y, Meyer AJ, and Dick TP. Real-time imaging of the intracellular glutathione redox potential. *Nat Methods* 5: 553–559, 2008.

78. Guzman JN, Sanchez-Padilla J, Wokosin D, Kondapalli J, Ilijic E, Schumacker PT, and Surmeier DJ. Oxidant stress evoked by pacemaking in dopaminergic neurons is attenuated by DJ-1. *Nature* 468: 696–700, 2010.

79. Haber F and Weiss J. The catalytic decomposition of hydrogen peroxide by iron salts. *Proc Royal Soc London A Math Phys Sci* 147: 332–351, 1934.

80. Halliwell B, Clement MV, and Long LH. Hydrogen peroxide in the human body. *FEBS Lett* 486: 10–13, 2000.

81. Han P, Ma N, Ren HF, Xu HP, Li ZB, Wang ZQ, and Zhang X. Oxidation-Responsive Micelles Based on a Selenium-Containing Polymeric Superamphiphile. *Langmuir* 26: 14414–14418, 2010.

82. Hanson GT, Aggeler R, Oglesbee D, Cannon M, Capaldi RA, Tsien RY, and Remington SJ. Investigating mitochondrial redox potential with redox-sensitive green fluorescent protein indicators. *J Biol Chem* 279: 13044–13053, 2004.

83. Hauptmann N, Grimsby J, Shih JC, and Cadenas E. The metabolism of tyramine by monoamine oxidase A/B causes oxidative damage to mitochondrial DNA. *Arch Biochem Biophys* 335: 295–304, 1996.

84. Hodge S, Hodge G, Holmes M, and Reynolds PN. Increased airway epithelial and T-cell apoptosis in COPD remains despite smoking cessation. *Eur Respir J* 25: 447–454, 2005.

85. Horoz M, Bolukbas C, Bolukbas FF, Aslan M, Koylu AO, Selek S, and Erel O. Oxidative stress in hepatitis C infected end-stage renal disease subjects. *BMC Infect Dis* 6, 2006.

86. Hruban Z, Hopkins E, Slesers A, and Vigil EL. Microbodies—constituent organelles of animal cells. *Lab Invest* 27: 184–191, 1972.

87. Ivashchenko O, Van Veldhoven PP, Brees C, Ho YS, Terlecky SR, and Fransen M. Intraperoxisomal redox balance in mammalian cells: oxidative stress and interorganellar cross-talk. *Mol Biol Cell* 22: 1440–1451, 2011.

88. Janczewski D, Song J, Csanyi E, Kiss L, Blazso P, Katona RL, Deli MA, Gros G, Xu JW, and Vancso GJ. Organometallic polymeric carriers for redox triggered release of molecular payloads. *J Mater Chem* 22: 6429–6435, 2012.

89. Kan W, Zhao K-s, Jiang Y, Yan W, Huang Q, Wang J, Qin Q, Huang X, and Wang S. Lung, spleen, and kidney are the major places for inducible nitric oxide synthase expression in endotoxic shock: role of p38 mitogen-activated protein kinase in signal transduction of inducible nitric oxide synthase expression. *Shock* 21: 281–287, 2004.

90. Karin M. Nuclear factor-kappaB in cancer development and progression. *Nature* 441: 431–436, 2006.

91. Keatings VM and Barnes PJ. Granulocyte activation markers in induced sputum: comparison between chronic obstructive pulmonary disease, asthma, and normal subjects. *Am J Respir Crit Care Med* 155: 449–453, 1997.

92. Keele BB, Mccord JM, and Fridovic I. Superoxide dismutase from *Escherichia-coli*-B - a new manganese-containing enzyme. *J Biol Chem* 245: 6176–6181, 1970.

93. Keller A, Mohamed A, Drose S, Brandt U, Fleming I, and Brandes RP. Analysis of dichlorodihydrofluorescein and dihydrocalcein as probes for the detection of intracellular reactive oxygen species. *Free Radic Res* 38: 1257–1267, 2004.

94. Kim JH, Chu SC, Gramlich JL, Pride YB, Babendreier E, Chauhan D, Salgia R, Podar K, Griffin JD, and Sattler M. Activation of the PI3K/mTOR pathway by BCR-ABL contributes to increased production of reactive oxygen species. *Blood* 105: 1717–1723, 2005.

95. Kim JY, Il Choi W, Kim YH, and Tae G. Highly selective *in-vivo* imaging of tumor as an inflammation site by ROS detection using hydrocyanine-conjugated, functional nano-carriers. *J Controlled Release* 156: 398–405, 2011.

96. Kinkade Jr JM, Pember SO, Barnes KC, Shapira R, Spitznagel JK, and Martin LE. Differential distribution of distinct forms of myeloperoxidase in different azurophilic granule subpopulations from human neutrophils. *Biochem Biophys Res Comm* 114: 296–303, 1983.

97. Kirkinezos IG and Moraes CT. Reactive oxygen species and mitochondrial diseases. *Semin Cell Dev Biol* 12: 449–457, 2001.

98. Kitazawa M, Anantharam V, and Kanthasamy AG. Dieldrin-induced oxidative stress and neurochemical changes contribute to apoptopic cell death in dopaminergic cells. *Free Radic Biol Med* 31: 1473–1485, 2001.

99. Klebanoff SJ. Myeloperoxidase: friend and foe. *J Leukocyte Biol* 77: 598–625, 2005.

100. Knowles RG and Moncada S. Nitric-oxide synthases in mammals. *Biochem J* 298: 249–258, 1994.

101. Kostikas K, Papatheodorou G, Psathakis K, Panagou P, and Loukides S. Oxidative stress in expired breath condensate of patients with COPD. *Chest* 124: 1373–1380, 2003.

102. Kotake S, Udagawa N, Takahashi N, Matsuzaki K, Itoh K, Ishiyama S, Saito S, Inoue K, Kamatani N, Gillespie MT, Martin TJ, and Suda T. IL-17 in synovial fluids from patients with rheumatoid arthritis is a potent stimulator of osteoclastogenesis. *J Clin Invest* 103: 1345–1352, 1999.

103. Kruth HS, Jones NL, Huang W, Zhao B, Ishii I, Chang J, Combs CA, Malide D, and Zhang WY. Macropinocytosis is the endocytic pathway that mediates macrophage foam cell formation with native low density lipoprotein. *J Biol Chem* 280: 2352–2360, 2005.

104. Kulbaba K, MacLachlan MJ, Evans CEB, and Manners I. Organometallic gels: Characterization and electrochemical studies of swellable, thermally crosslinked poly(ferrocenylsilane)s. *Macromol Chem Phys* 202: 1768–1775, 2001.

105. Kundu K, Knight SF, Willett N, Lee S, Taylor WR, and Murthy N. Hydrocyanines: A class of fluorescent sensors that can image reactive oxygen species in cell culture, tissue, and in vivo. *Angew Chem Int Edit* 48: 299–303, 2009.

106. Kuwana Y, Takei M, Yajima M, Imadome K, Inomata H, Shiozaki M, Ikumi N, Nozaki T, Shiraiwa H, Kitamura N, Takeuchi J, Sawada S, Yamamoto N, Shimizu N, Ito M, and Fujiwara S. Epstein-Barr virus induces erosive arthritis in humanized mice. *PLoS One* 6: e26630, 2011.

107. Kwon NS, Nathan CF, Gilker C, Griffith OW, Matthews DE, and Stuehr DJ. L-citrulline production from L-arginine by macrophage nitric oxide synthase. The ureido oxygen derives from dioxygen. *J Biol Chem* 265: 13442–13445, 1990.

108. Labunskyy VM and Gladyshev VN. Role of reactive oxygen species-mediated signaling in aging. *Antioxid Redox Signal* 19: 1362–1372, 2012.

109. Lacy F, Gough DA, and Schmid-Schonbein GW. Role of xanthine oxidase in hydrogen peroxide production. *Free Radic Biol Med* 25: 720–727, 1998.

110. Lee D, Bae S, Hong D, Lim H, Yoon JH, Hwang O, Park S, Ke Q, Khang G, and Kang PM. H_2O_2-responsive molecularly engineered polymer nanoparticles as ischemia/reperfusion-targeted nanotherapeutic agents. *Sci Rep* 3: 2233, 2013.

111. Lee D, Khaja S, Velasquez-Castano JC, Dasari M, Sun C, Petros J, Taylor WR, and Murthy N. *In vivo* imaging of hydrogen peroxide with chemiluminescent nanoparticles. *Nat Mater* 6: 765–769, 2007.

112. Lee SH, Gupta MK, Bang JB, Bae H, and Sung HJ. Current progress in reactive oxygen species (ROS)-responsive materials for biomedical applications. *Adv Healthcare Mater* 2: 908–915, 2013.

113. Li DW, Qin LX, Li Y, Nia RP, Long YT, and Chen HY. CdSe/ZnS quantum dot-Cytochrome c bioconjugates for selective intracellular O_2 (-) sensing. *Chem Commun (Camb)* 47: 8539–8541, 2011.

114. Li X and Makarov SS. An essential role of NF-kappaB in the ''tumor-like'' phenotype of arthritic synoviocytes. *Proc Natl Acad Sci U S A* 103: 17432–17437, 2006.

115. Lim CK, Lee YD, Na J, Oh JM, Her S, Kim K, Choi K, Kim S, and Kwon IC. Chemiluminescence-generating nanoreactor formulation for near-infrared imaging of hydrogen peroxide and glucose level *in vivo. Adv Funct Mater* 20: 2644–2648, 2010.

116. Ling LU, Tan KB, Lin H, and Chiu GN. The role of reactive oxygen species and autophagy in safingol-induced cell death. *Cell Death Dis* 2: e129, 2011.

117. Liou GY and Storz P. Reactive oxygen species in cancer. *Free Radic Res* 44: 479–496, 2010.

118. Liu Q, Berchner-Pfannschmidt U, Möller U, Brecht M, Wotzlaw C, Acker H, Jungermann K, and Kietzmann T. A Fenton reaction at the endoplasmic reticulum is involved in the redox control of hypoxia-inducible gene expression. *Proc Natl Acad Sci USA* 101: 4302–4307, 2004.

119. Liu W, Vives-Bauza C, Acin-Perez R, Yamamoto A, Tan Y, Li Y, Magrane J, Stavarache MA, Shaffer S, Chang S, Kaplitt MG, Huang XY, Beal MF, Manfredi G, and Li C. PINK1 defect causes mitochondrial dysfunction, proteasomal deficit and alpha-synuclein aggregation in cell culture models of Parkinson's disease. *PLoS One* 4: e4597, 2009.

120. Lu C, Song G, and Lin J-M. Reactive oxygen species and their chemiluminescence-detection methods. *TrAC Trends Anal Chem* 25: 985–995, 2006.

121. Ma N, Li Y, Ren HF, Xu HP, Li ZB, and Zhang X. Selenium-containing block copolymers and their oxidation-responsive aggregates. *Polymer Chem* 1: 1609–1614, 2010.

122. Ma N, Li Y, Xu HP, Wang ZQ, and Zhang X. Dual redox responsive assemblies formed from diselenide block copolymers. *J Am Che Soc* 132: 442–443, 2010.

123. Ma N, Xu HP, An LP, Li J, Sun ZW, and Zhang X. Radiation-sensitive diselenide block co-polymer micellar aggregates: toward the combination of radiotherapy and chemotherapy. *Langmuir* 27: 5874–5878, 2011.

124. Mahdi H, Fisher BA, Kallberg H, Plant D, Malmstrom V, Ronnelid J, Charles P, Ding B, Alfredsson L, Padyukov L, Symmons DP, Venables PJ, Klareskog L, and Lundberg K. Specific interaction between genotype, smoking and autoimmunity to citrullinated alpha-enolase in the etiology of rheumatoid arthritis. *Nat Genet* 41: 1319–1324, 2009.

125. Mahmoud EA, Sankaranarayanan J, Morachis JM, Kim G, and Almutairi A. Inflammation responsive logic gate nanoparticles for the delivery of proteins. *Bioconj Chem* 22: 1416–1421, 2011.

126. Malerba M, Ricciardolo F, Radaeli A, Torregiani C, Ceriani L, Mori E, Bontempelli M, Tantucci C, and Grassi V. Neutrophilic inflammation and IL-8 levels in induced sputum of alpha-1-antitrypsin PiMZ subjects. *Thorax* 61: 129–133, 2006.

127. Malinouski M, Zhou Y, Belousov VV, Hatfield DL, and Gladyshev VN. Hydrogen peroxide probes directed to different cellular compartments. *PLoS One* 6, 2011.

128. Martinez-Ruiz A and Lamas S. Signalling by NO-induced protein S-nitrosylation and S-glutathionylation: convergences and divergences. *Cardiovasc Res* 75: 220–228, 2007.

129. Mccord JM and Fridovic.I. Superoxide dismutase an enzymic function for erythrocuprein (Hemocuprein). *J Biol Chem* 244: 6049–6055, 1969.

130. Meyer AJ, Brach T, Marty L, Kreye S, Rouhier N, Jacquot JP, and Hell R. Redox-sensitive GFP in Arabidopsis thaliana is a quantitative biosensor for the redox potential of the cellular glutathione redox buffer. *Plant J* 52: 973–986, 2007.

131. Michiko Sukenobu H, Horiike K, Tojo H, Katagiri M, and Yamano T. Kinetic properties of rat kidney d-amino acid oxidase associated with peroxisomes. *Comp Biochem Physiol B Comp Biochem* 80: 425–430, 1985.

132. Miller EW, Albers AE, Pralle A, Isacoff EY, and Chang CJ. Boronate-based fluorescent probes for imaging cellular hydrogen peroxide. *J Am Chem Soc* 127: 16652–16659, 2005.

133. Mills GC. Hemoglobin catabolism: I. glutathione peroxidase, an erythrocyte enzyme which protects hemoglobin from oxidative breakdown. *J Biol Chem* 229: 189–197, 1957.

134. Mohanty JG, Jaffe JS, Schulman ES, and Raible DG. A highly sensitive fluorescent micro-assay of H_2O_2 release from activated human leukocytes using a dihydroxyphenoxazine derivative. *J Immunol Methods* 202: 133–141, 1997.

135. Morgan EJ. The distribution of xanthine oxidase I. *Biochem J* 20: 1282–1291, 1926.

136. Moss DW and Bates TE. Activation of murine microglial cell lines by lipopolysaccharide and interferon-gamma causes NO-mediated decreases in mitochondrial and cellular function. *Eur J Neurosci* 13: 529–538, 2001.

137. Nadel JA. Role of neutrophil elastase in hypersecretion during COPD exacerbations, and proposed therapies. *Chest* 117: 386S–389S, 2000.

138. Nakahata M, Takashima Y, Yamaguchi H, and Harada A. Redox-responsive self-healing materials formed from host-guest polymers. *Nat Comm* 2, 2011.

139. Napoli A, Valentini M, Tirelli N, Muller M, and Hubbell JA. Oxidation-responsive polymeric vesicles. *Nat Mat* 3: 183–189, 2004.

140. Nathan C and Shiloh MU. Reactive oxygen and nitrogen intermediates in the relationship between mammalian hosts and microbial pathogens. *Proc Natl Acad Sci U S A* 97: 8841–8848, 2000.

141. Ohashi T, Mizutani A, Murakami A, Kojo S, Ishii T, and Taketani S. Rapid oxidation of dichlorodihydrofluorescin with heme and hemoproteins: formation of the fluorescein is independent of the generation of reactive oxygen species. *FEBS Lett* 511: 21–27, 2002.

142. Ostergaard H, Henriksen A, Hansen FG, and Winther JR. Shedding light on disulfide bond formation: engineering a redox switch in green fluorescent protein. *EMBO J* 20: 5853–5862, 2001.

143. Oushiki D, Kojima H, Terai T, Arita M, Hanaoka K, Urano Y, and Nagano T. Development and application of a near-infrared fluorescence probe for oxidative stress based on differential reactivity of linked cyanine dyes. *J Am Chem Soc* 132: 2795–2801, 2010.

144. Owusu-Ansah E, Yavari A, and Banerjee U. A protocol for *in vivo* detection of reactive oxygen species. *Protocol Exchange* 2008. [Epub ahead of print]; DOI:10.1038/nprot.2008.23.

145. Page G, Lebecque S, and Miossec P. Anatomic localization of immature and mature dendritic cells in an ectopic lymphoid organ: correlation with selective chemokine expression in rheumatoid synovium. *J Immunol* 168: 5333–5341, 2002.

146. Palacino JJ, Sagi D, Goldberg MS, Krauss S, Motz C, Wacker M, Klose J, and Shen J. Mitochondrial dysfunction and oxidative damage in parkin-deficient mice. *J Biol Chem* 279: 18614–18622, 2004.

147. Parge HE, Hallewell RA, and Tainer JA. Atomic structures of wild-type and thermostable mutant recombinant human Cu,Zn superoxide-dismutase. *Proc Natl Acad Sci U S A* 89: 6109–6113, 1992.

148. Rajagopalan S, Meng XP, Ramasamy S, Harrison DG, and Galis ZS. Reactive oxygen species produced by macrophage-derived foam cells regulate the activity of vascular matrix metalloproteinases *in vitro*. Implications for atherosclerotic plaque stability. *J Clin Invest* 98: 2572–2579, 1996.

149. Rehor A, Hubbell JA, and Tirelli N. Oxidation-sensitive polymeric nanoparticles. *Langmuir* 21: 411–417, 2005.

150. Ren HF, Wu YT, Ma N, Xu HP, and Zhang X. Side-chain selenium-containing amphiphilic block copolymers: redox-controlled self-assembly and disassembly. *Soft Matter* 8: 1460–1466, 2012.

151. Robertson RP. Chronic oxidative stress as a central mechanism for glucose toxicity in pancreatic islet beta cells in diabetes. *J Biol Chem* 279: 42351–42354, 2004.

152. Rohnstock A and Lehmann L. Evaluation of the probe dihydrocalcein acetoxymethylester as an indicator of reactive oxygen species formation and comparison with oxidative DNA base modification determined by modified alkaline elution technique. *Toxicol In Vitro* 21: 1552–1562, 2007.

153. Rosen DR, Siddique T, Patterson D, Figlewicz DA, Sapp P, Hentati A, Donaldson D, Goto J, O'Regan JP, Deng HX, *et al.* Mutations in Cu/Zn superoxide dismutase gene are associated with familial amyotrophic lateral sclerosis. *Nature* 362: 59–62, 1993.

154. Royall JA and Ischiropoulos H. Evaluation of 2′,7′-dichlorofluorescin and dihydrorhodamine 123 as fluorescent probes for intracellular H_2O_2 in cultured endothelial cells. *Arch Biochem Biophys* 302: 348–355, 1993.

155. Saetta M, Baraldo S, Corbino L, Turato G, Braccioni F, Rea F, Cavallesco G, Tropeano G, Mapp CE, Maestrelli P, Ciaccia A, and Fabbri LM. CD8 + ve cells in the lungs of smokers with chronic obstructive pulmonary disease. *Am J Respir Crit Care Med* 160: 711–717, 1999.

156. Schirmer RH, Schulz GE, and Untuchtgrau R. On the geometry of leukocyte nadph-oxidase, a membrane flavoenzyme—inferences from the structure of glutathione-reductase. *FEBS Lett* 154: 1–4, 1983.

157. Schrijvers DM, De Meyer GR, Kockx MM, Herman AG, and Martinet W. Phagocytosis of apoptotic cells by macrophages is impaired in atherosclerosis. *Arterioscler Thromb Vasc Biol* 25: 1256–1261, 2005.

158. Seifried HE, Anderson DE, Fisher EI, and Milner JA. A review of the interaction among dietary antioxidants and reactive oxygen species. *J Nutr Biochem* 18: 567–579, 2007.

159. Seimon TA, Nadolski MJ, Liao X, Magallon J, Nguyen M, Feric NT, Koschinsky ML, Harkewicz R, Witztum JL, Tsimikas S, Golenbock D, Moore KJ, and Tabas I. Atherogenic lipids and lipoproteins trigger CD36-TLR2-dependent apoptosis in macrophages undergoing endoplasmic reticulum stress. *Cell Metab* 12: 467–482, 2010.

160. Sem X and Rhen M. Pathogenicity of *Salmonella enterica* in *Caenorhabditis elegans* relies on disseminated oxidative stress in the infected host. *PLoS One* 7: e45417, 2012.

161. Shigenaga MK, Hagen TM, and Ames BN. Oxidative damage and mitochondrial decay in aging. *Proc Natl Acad Sci U S A* 91: 10771–10778, 1994.

162. Shim MS and Xia Y. A reactive oxygen species (ROS)-responsive polymer for safe, efficient, and targeted gene delivery in cancer cells. *Angew Chem Int Ed Engl* 52: 6926–6929, 2013.

163. Simonson SG, Zhang J, Canada AT, Jr., Su YF, Benveniste H, and Piantadosi CA. Hydrogen peroxide production by monoamine oxidase during ischemia-reperfusion in the rat brain. *J Cereb Blood Flow Metab* 13: 125–134, 1993.

164. Slot JW, Geuze HJ, Freeman BA, and Crapo JD. Intracellular localization of the copper-zinc and manganese superoxide dismutases in rat liver parenchymal cells. *Lab Invest* 55: 363–371, 1986.

165. Snir O, Widhe M, von Spee C, Lindberg J, Padyukov L, Lundberg K, Engstrom A, Venables PJ, Lundeberg J, Holmdahl R, Klareskog L, and Malmstrom V. Multiple antibody reactivities to citrullinated antigens in sera from patients with rheumatoid arthritis: association with HLA-DRB1 alleles. *Ann Rheum Dis* 68: 736–743, 2009.

166. Stadtman ER and Levine RL. Free radical-mediated oxidation of free amino acids and amino acid residues in proteins. *Amino Acids* 25: 207–218, 2003.

167. Staff RH, Gallei M, Mazurowski M, Rehahn M, Berger R, Landfester K, and Crespy D. Patchy nanocapsules of poly(vinylferrocene)-based block copolymers for redox-responsive release. *ACS Nano* 6: 9042–9049, 2012.

168. Starkov AA, Fiskum G, Chinopoulos C, Lorenzo BJ, Browne SE, Patel MS, and Beal MF. Mitochondrial alpha-ketoglutarate dehydrogenase complex generates reactive oxygen species. *J Neurosci* 24: 7779–7788, 2004.

169. Stolz DB, Zamora R, Vodovotz Y, Loughran PA, Billiar TR, Kim Y-M, Simmons RL, and Watkins SC. Perox-

isomal localization of inducible nitric oxide synthase in hepatocytes. *Hepatology* 36: 81–93, 2002.

170. Strålin P, Karlsson K, Johansson BO, and Marklund SL. The interstitium of the human arterial wall contains very large amounts of extracellular superoxide dismutase. *Arterioscler Thromb Vasc Biol* 15: 2032–2036, 1995.

171. Szatrowski TP and Nathan CF. Production of Large Amounts of Hydrogen-Peroxide by Human Tumor-Cells. *Cancer Res* 51: 794–798, 1991.

172. Tabor CW, Tabor H, and Rosenthal SM. Purification of Amine Oxidase From Beef Plasma. *J Biol Chem* 208: 645–662, 1954.

173. Takahashi K, Avissar N, Whitin J, and Cohen H. Purification and characterization of human-plasma glutathione-peroxidase - a selenoglycoprotein distinct from the known cellular enzyme. *Arch Biochem Biophys* 256: 677–686, 1987.

174. Taylor RW and Turnbull DM. Mitochondrial DNA mutations in human disease. *Nat Rev Genet* 6: 389–402, 2005.

175. Tedgui A and Mallat Z. Cytokines in atherosclerosis: pathogenic and regulatory pathways. *Physiol Rev* 86: 515–581, 2006.

176. Teitelbaum SL. Bone resorption by osteoclasts. *Science* 289: 1504–1508, 2000.

177. Teoh ML, Fitzgerald MP, Oberley LW, and Domann FE. Overexpression of extracellular superoxide dismutase attenuates heparanase expression and inhibits breast carcinoma cell growth and invasion. *Cancer Res* 69: 6355–6363, 2009.

178. Test ST and Weiss SJ. Quantitative and temporal characterization of the extracellular H_2O_2 pool generated by human neutrophils. *J Biol Chem* 259: 399–405, 1984.

179. Thomas C, Mackey MM, Diaz AA, and Cox DP. Hydroxyl radical is produced via the Fenton reaction in submitochondrial particles under oxidative stress: implications for diseases associated with iron accumulation. *Redox Report* 14: 102–108, 2009.

180. Thomas DD, Ridnour LA, Isenberg JS, Flores-Santana W, Switzer CH, Donzelli S, Hussain P, Vecoli C, Paolocci N, Ambs S, Colton CA, Harris CC, Roberts DD, and Wink DA. The chemical biology of nitric oxide: implications in cellular signaling. *Free Radic Biol Med* 45: 18–31, 2008.

181. Turrens JF and Boveris A. Generation of superoxide anion by the NADH dehydrogenase of bovine heart mitochondria. *Biochem J* 191: 421–427, 1980.

182. Urao N and Ushio-Fukai M. Redox regulation of stem/ progenitor cells and bone marrow niche. *Free Radic Biol Med* 54: 26–39, 2013.

183. Uusitalo LM and Hempel N. Recent advances in intracellular and in vivo ROS sensing: focus on nanoparticle and nanotube applications. *Int J Mol Sci* 13: 10660–10679, 2012.

184. Vafa O, Wade M, Kern S, Beeche M, Pandita TK, Hampton GM, and Wahl GM. c-Myc can induce DNA damage, increase reactive oxygen species, and mitigate p53 function: a mechanism for oncogene-induced genetic instability. *Mol Cell* 9: 1031–1044, 2002.

185. Van de Bittner GC, Dubikovskaya EA, Bertozzi CR, and Chang CJ. *In vivo* imaging of hydrogen peroxide production in a murine tumor model with a chemoselective bioluminescent reporter. *Proc Natl Acad Sci U S A*, 107: 21316–21321, 2010.

186. van Lith M, Tiwari S, Pediani J, Milligan G, and Bulleid NJ. Real-time monitoring of redox changes in the mammalian endoplasmic reticulum. *J Cell Sci* 124: 2349–2356.

187. Van Remmen H, Ikeno Y, Hamilton M, Pahlavani M, Wolf N, Thorpe SR, Alderson NL, Baynes JW, Epstein CJ, Huang TT, Nelson J, Strong R, and Richardson A. Lifelong reduction in MnSOD activity results in increased DNA damage and higher incidence of cancer but does not accelerate aging. *Physiol Genomics* 16: 29–37, 2003.

188. Viger ML, Sankaranarayanan J, de Gracia Lux C, Chan M, and Almutairi A. Collective activation of MRI agents via encapsulation and disease-triggered release. *J Am Chem Soc* 135: 7847–7850, 2013.

189. Villela GG, Mitidieri E, and Affonso OR. Intracellular Distribution of Xanthine Oxidase in the Rat Liver. *Nature* 175: 1087–1087, 1955.

190. Vong LB, Tomita T, Yoshitomi T, Matsui H, and Nagasaki Y. An orally administered redox nanoparticle that accumulates in the colonic mucosa and reduces colitis in mice. *Gastroenterology* 143: 1027–1036 e3, 2012.

191. Votyakova TV and Reynolds IJ. Detection of hydrogen peroxide with Amplex Red: interference by NADH and reduced glutathione auto-oxidation. *Arch Biochem Biophys* 431: 138–144, 2004.

192. Wegner N, Wait R, Sroka A, Eick S, Nguyen KA, Lundberg K, Kinloch A, Culshaw S, Potempa J, and Venables PJ. Peptidylarginine deiminase from Porphyromonas gingivalis citrullinates human fibrinogen and alpha-enolase: implications for autoimmunity in rheumatoid arthritis. *Arthritis Rheum* 62: 2662–2672, 2010.

193. Weisiger RA and Fridovich I. Superoxide dismutase. Organelle specificity. *J Biol Chem* 248: 3582–3592, 1973.

194. Wheeler MD, Smutney OM, and Samulski RJ. Secretion of extracellular superoxide dismutase from muscle transduced with recombinant adenovirus inhibits the growth of B16 melanomas in mice. *Mol Cancer Res* 1: 871–881, 2003.

195. Williams KJ and Tabas I. The response-to-retention hypothesis of early atherogenesis. *Arterioscler Thromb Vasc Biol* 15: 551–561, 1995.

196. Wilson DS, Dalmasso G, Wang LX, Sitaraman SV, Merlin D, and Murthy N. Orally delivered thioketal nanoparticles loaded with TNF-alpha-siRNA target inflammation and inhibit gene expression in the intestines. *Nat Mater* 9: 923–928, 2010.

197. Wong A, Yang J, Cavadini P, Gellera C, Lonnerdal B, Taroni F, and Cortopassi G. The Friedreich's ataxia mutation confers cellular sensitivity to oxidant stress which is rescued by chelators of iron and calcium and inhibitors of apoptosis. *Hum Mol Genet* 8: 425–430, 1999.

198. Wu EC, Park JH, Park J, Segal E, Cunin F, and Sailor MJ. Oxidation-triggered release of fluorescent molecules or drugs from mesoporous Si microparticles. *ACS Nano* 2: 2401–2409, 2008.

199. Yamada H and Yasunobu KT. Monoamine oxidase - purification, crystallization, and properties of plasma monoamine oxidase. *J Biol Chem* 237: 1511–1516, 1962.

200. Yan Q, Yuan JY, Cai ZN, Xin Y, Kang Y, and Yin YW. Voltage-Responsive Vesicles Based on Orthogonal Assembly of Two Homopolymers. *J Am Chem Soc* 132: 9268–9270, 2010.

201. Yano T, Oku M, Akeyama N, Itoyama A, Yurimoto H, Kuge S, Fujiki Y, and Sakai Y. A novel fluorescent sensor protein for visualization of redox states in the cytoplasm and in peroxisomes. *Mol Cell Biol* 30: 3758–3766, 2010.

202. Yu SS, Koblin RL, Zachman AL, Perrien DS, Hofmeister LH, Giorgio TD, and Sung HJ. Physiologically relevant

oxidative degradation of oligo(proline) cross-linked poly-meric scaffolds. *Biomacromolecules* 12: 4357–4366, 2011.

203. Zhang J, Fitsanakis VA, Gu G, Jing D, Ao M, Amarnath V, and Montine TJ. Manganese ethylene-bis-dithiocarbamate and selective dopaminergic neurodegeneration in rat: a link through mitochondrial dysfunction. *J Neurochem* 84: 336–346, 2003.

204. Zhao H, Joseph J, Fales HM, Sokoloski EA, Levine RL, Vasquez-Vivar J, and Kalyanaraman B. Detection and characterization of the product of hydroethidine and intra-cellular superoxide by HPLC and limitations of fluorescence. *Proc Natl Acad Sci U S A* 102: 5727–5732, 2005.

205. Zhou MJ, Diwu ZJ, PanchukVoloshina N, and Haugland RP. A stable nonfluorescent derivative of resorufin for the fluoro-metric determination of trace hydrogen peroxide: applications in detecting the activity of phagocyte NADPH oxidase and other oxidases. *Anal Biochem* 253: 162–168, 1997.

206. Zhu MT, Nie GJ, Meng H, Xia T, Nel A, and Zhao YL. Physicochemical properties determine nanomaterial cel-lular uptake, transport, and fate. *Acc Chem Res* 46: 622–631, 2013.

Address correspondence to:
Prof. Adah Almutairi
Skaggs School of Pharmacy and Pharmaceutical Sciences
KACST-UCSD Center of Excellence in Nanomedicine
Laboratory of Bioresponsive Materials
University of California
San Diego, CA-92093

E-mail: aalmutairi@ucsd.edu

Abbreviations Used

β-CD = beta cyclodextrin
ALS = amyotrophic lateral sclerosis
Bcr-Abl = Breakpoint cluster region- Abelson murine leukemia
CD8$^+$ = cluster of differentiation 8 positive
CoA = coenzyme A
COPD = chronic obstructive pulmonary disease
cPCL = poly(carboxy-ε-caprolactone)
CPO = chloroperoxidase
cpYFP = circularly permuted yellow fluorescent protein
DCFH-DA = 2'-7'-dichlorodihydrofluorescein diacetate
DiO = (3,3'-dioctadecyloxacarbocyanine perchlorate)
DLS = dynamic light scattering
DMA = N,N-dimethylacrylamide
DNA = deoxyribonucleic acid
DOTAP = 1,2-dioleoyl-3-trimethylammonium-propane
Dox = doxorubicin
DSC = differential scanning calorimetry
ECM = extracellular matrix
EC-SOD = extracellular superoxide dismutase
EG = ethylene glycol

ER = endoplasmic reticulum
ETC = electron transport chain
Fc = ferrocenyl group
Fc$^+$ = ferrocenium ion
FluNa = fluorescein sodium
FTIR = Fourier transform infrared spectroscopy
GFP = green fluorescent protein
GPC = gel permeation chromatography
GPX = glutathione peroxidase
GRP78 = glucose-regulated protein 78
GRX = glutaredoxin
GSH = glutathione
H$_2$DCFDA = dichlorodihydrofluorescein diacetate
HE = hydroethidine
HLB = hydrophilic to lipophilic balance
hMPO = human myeloperoxidase
IFNγ = interferon gamma
IL-1 = interleukin-1
K_a = association constant
Mn = number average molecular weight
MMP = matrix metalloproteinase
MPO = myeloperoxidase
MPRO = mouse promyelocyte
mRNA = messenger ribonucleic acid
mt DNA = mitochondrial DNA
mtNOS = mitochondrial nitric oxide synthase
NADPH = nicotinamide adenine dinucleotide phosphate
NC = nanocapsule
NMR = nuclear magnetic resonance
NOS = nitric oxide synthase
NOX = nicotinamide adenine dinucleotide phos-phate oxidase
NP = nanoparticle
NR = Nile red
OD = optical density
OVA = ovalbumin Alexa Fluor 594
pAA = poly(acrylic acid)
pAA-β-CD = poly(acrylic acid) containing 4%–5% substitution of the COOH by beta cyclodextrins
pAA-Fc = poly(acrylic acid) containing 2.7% substitution of the COOH by ferrocene groups
PBS = phosphate-buffered saline
PCL = poly(ε-caprolactone)
PD = Parkinson's disease
PEG = poly(ethylene glycol)
PGSE = pulse gradient spin echo
PINK1 = phosphatase and tensin homolog-induced putative kinase 1
PLGA = poly(lactic-*co*-glycolic) acid
PMNs = polymorphonuclear leukocytes
Pn = proline oligomer
PPADT = poly-(1,4-phenyleneacetone dimethylene thioketal)
PPS = poly(propylene sulfide)
PS = propylene sulfide
PVAX = copolyoxylate containing vanillyl alcohol
PVFc = poly(vinylferrocene)
PVFc-*b*-PMMA = poly(vinylferrocene)-block-poly(methyl methacrylate)

Abbreviations Used (Cont.)

RA = rheumatoid arthritis
RB = rhodamine B
ROS = reactive oxygen species
RNP^O = redox nanoparticle
RNS = reactive nitrogen species
roGFP = redox-sensitive green fluorescent protein
rxYFP = redox-sensitive yellow fluorescent protein
SeQTA = selenium-containing surfactant
SIN-1 = morpholinosydnonimine
siRNA = small interfering ribonucleic acid

SIRS = systemic inflammatory response syndrome
SOD = superoxide dismutase
T_H17 cells = autoantigen-sensitized T cells
TEM = transmission electron microscopy
TEMPOL = 4-hydroxy-2,2,6,6-tetramethylpiperidin-1-oxyl
TKN = thioketal nanoparticle
TNFα = tumor necrosis factor alpha
VA = vanillyl alcohol
XPS = X-ray photoelectron spectroscopy
YFP = yellow fluorescent protein